ISAS - INTERNATIONAL SCHOOL FOR ADVANCED STUDIES

SCALING BEHAVIOR FOR MODELS OF RIVER NETWORK

Thesis submitted for the degree of
"Doctor Philosophiæ"

CANDIDATE

Alessandro Flammini

SUPERVISOR

Prof. Amos Maritan

October 1996

SISSA - SCUOLA NTERNAZIONALE SUPERIORE I STUDI AVANZATI
TRIESTE
Strada Costiera 11

TRIESTE

Table of Contents

List of Figures

1 Introduction

One of the most fascinating subject in Statistical Mechanics in the last 30 years has been the critical phenomena and their feature of scale invariance and universality.

Roughly speaking scale invariance is the property of systems at critical point to exhibit the same characteristics at different space and time scales. Lot of these systems, despite of their different nature, have the same scale invariance property, i.e they are characterized by the same critical exponents. This feature is generally called universality, meaning independence of the scaling behavior on the details of the interactions between effective degrees of freedom of the system.

Scale invariance and universality are not a prerogative of critical phenomena. Many other systems in Nature share the same features without the need to set any parameters on critical values as happens for example in ferromagnetic materials with the temperature and the magnetic field.

River basins are a beautiful example of systems in which the properties of scale invariance have been neatly observed over several order of magnitude [1, 2, 3, 4]. Moreover these properties demonstrated to be quantitatively unaffected by change in climate, lithology and ubication, showing in this sense a strong universal behavior.

Aim of this work is to extend some ideas like finite size scaling, scaling relations and universality classes which demonstrates so powerful in the context of critical phenomena for the study of river networks.

Fluvial systems are encountered in the most different environmental conditions, they have sizes which goes from few to thousands kilometers, therein myriad of processes which act in a wide range of spatial and temporal scales are involved, thus it would appear a difficult task to describe the structure of river basin and its evolution.

In an early contribution toward the understanding of landscape evolution [5], Leopold et *al.* argued that because the number of features affecting the landscape evolution is exceedingly large, any realistic coupled model of hillslope, channel network and river basin needs to be complex.

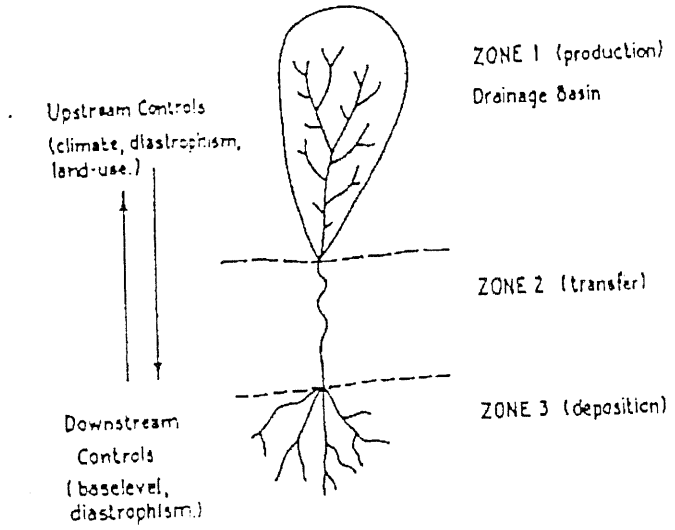

Figure 1.1: Idealized fluvial system (after Schumm [1977])

Nevertheless in those years lot of similarities began to be observed in river networks, giving the feeling that, despite of their complexity, some simple mechanism could be invoked to explain the quantitative similarities between different river basins.

Before going ahead we need to better specify what we intend for river basin.

1.1 River Basin

The whole picture of a river system may be divided in three loosely separated, nevertheless distinct regions.

They are shown in figure (1.1) and according to their mean working purpose they are called, following Schumm [6], the production zone, the transport or transfer zone and the delivery or deposition zone.

The production zone is what we call river basin. This is the zone in which the river originates collecting the most part of precipitation and of sediments which are then transferred through the plain to their final delivery to oceans.

This zone is described in terms of two deeply interrelated elements: the two-dimensional structure of channel network, i.e. the set of all rivulets through which water is drained and that coalesce to give place to what is generally meant to be a river, and the underlying three-dimensional structure of hillslope. The hillslope drives water like a constraint and at the same time, by mean of erosion and of deposition of eroded material is modified and

rearranged by water.

The mutual interaction between hillslope and channel network make this system extremely hard to study from the experimental point of view. Two have been the main difficulties: the first is that evolution takes place on time scales which are extremely long with respect to human life, leaving only the possibility to consider basins of different ages but in completely different environmental conditions; the second is that for a long time also the three-dimensional structure of hillslope resulted inaccessible to accurate and extensive measurements. That's why the earlier works one can find in the literature, both experimental and theoryc regard almost exclusively the bidimensional structure of channel networks.

The situation changed radically with the introduction of Digital Elevation Maps (DEM) that we describe in the next Section.

1.2 Digital Elevation Maps

Digital Elevation Maps (DEM) are discretized reconstruction of the three dimensional structure of hillslope by mean of aerial topography [7, 8].

From a satellite several photographs are taken of a given landscape. The plan area underlying the landscape is ideally divided in square cells of about $30m$ side. To each cell is then associated a variable h_i equal to the mean height of the landscape in that cell.

In this way the observational data are simply translated into a field of elevations h_i on a lattice. Given that, the bidimensional drainage structure is reconstructed assuming that water flows in the direction of the steepest descent, i.e. assigning to each site i an outcoming link going from i to its nearest neighbor with smallest height, see figure (1.2). In figure (1.3) the set of drainage directions reconstructed from DEM is shown for a river in northern Italy, the Fella river.

The set of all drainage directions is a coarse grained but faithful representation of the bidimensional structure of a river network.

One point need to be clarified and it is the distinction between the drainage network and the water streams or channels: the links in the drainage network represent the directions of the path that water incoming in the system by precipitation follows to reach the outlet, but not all of them represent channels, i.e. streams of real rivers. Channels may be identified with the set of sites through which the flow is above a given threshold. In the following drainage network and channel network will be used as synonymous, always referring to the set of drainage directions defined above.

If no lakes are present in the landscape, i.e. points in which all nearest neighbors have greater height, and it seems to be the case in the river production zone, the set of drainage

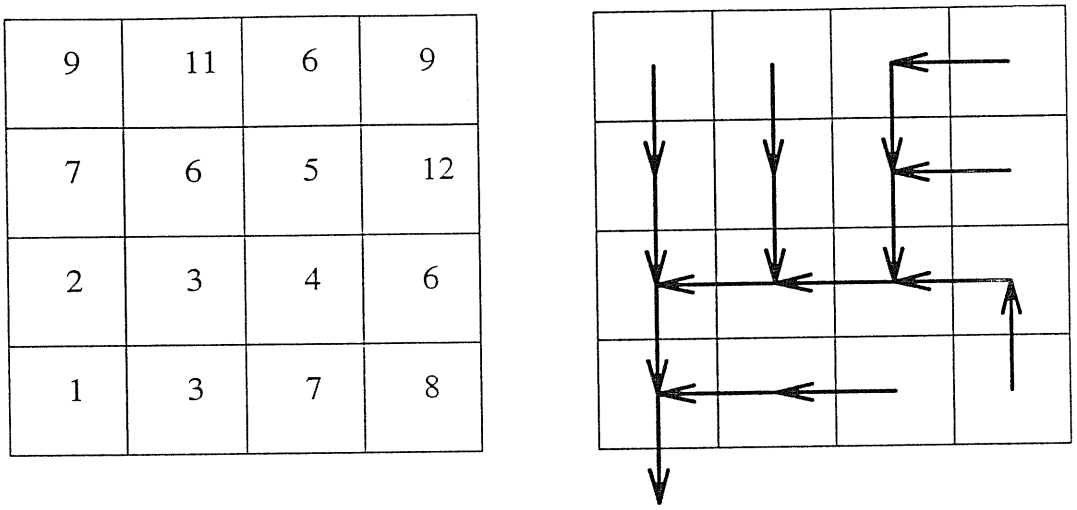

Figure 1.2: A field of elevation and the corresponding map of drainage directions

directions will be an oriented spanning tree, in which all vertices are connected to a common point (the outlet) through a unique oriented path. In this framework we say that site j is upstream with respect to site i if i is along the oriented path going from site j to the outlet.

Once the set of drainage directions is given, several quantities can be computed. We here define, in the context of DEM, two of these that are most commonly considered to describe the geometrical features of channel networks. In the next Section we will discuss the empirical evidences about them which emerge from DEM's data.

In the framework of a lattice representation of river basins we define the drained (or cumulated) area A_i at site i as the number of sites in the lattice which are upstream with respect to i. Variables A_i can be regarded also as the quantity of water flowing into i if a unit of precipitation is assumed at each site. Variables A_i result to be related by

$$A_i = A_j w_{ij} + 1 \tag{1.1}$$

where $\omega_{i,j}$ is 1 if and only if site i and site j are nearest neighbor and site j is upstream respect to site i. Figure (1.4) shows a small map of drainage directions and the value of variable A_i in each site.

The main stream length l_i at site i is defined as

$$l_i = \max_{j \in up(i)} d_{ij} \tag{1.2}$$

where d_{ij} is the distance between site i and site j along the spanning tree and index j runs over all sites which are upstream respect to i. In figure (1.5) the values of the mainstream length in a small map of drainage directions are shown.

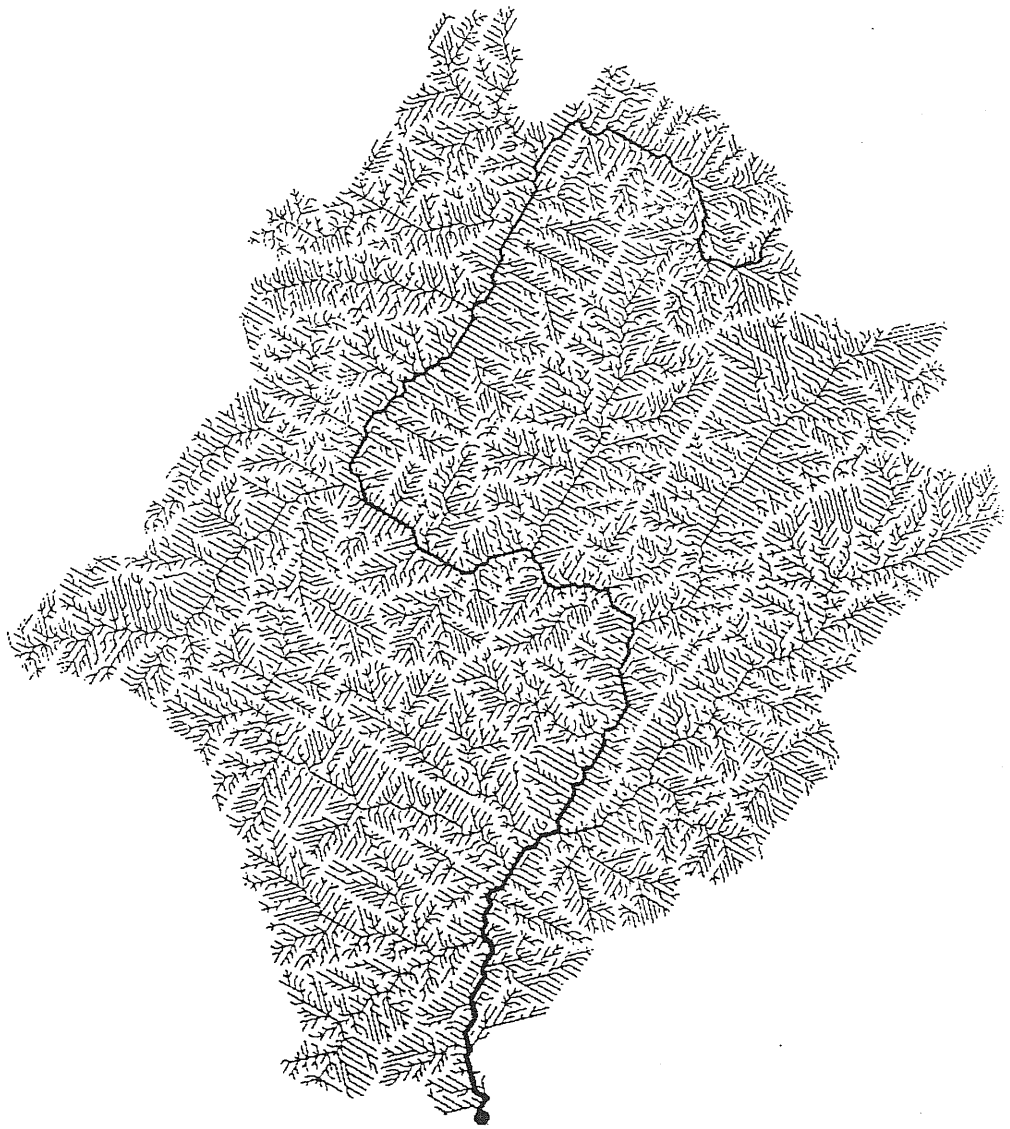

Figure 1.3: The set of drainage directions extract from DEM of Fella river in northern Italy

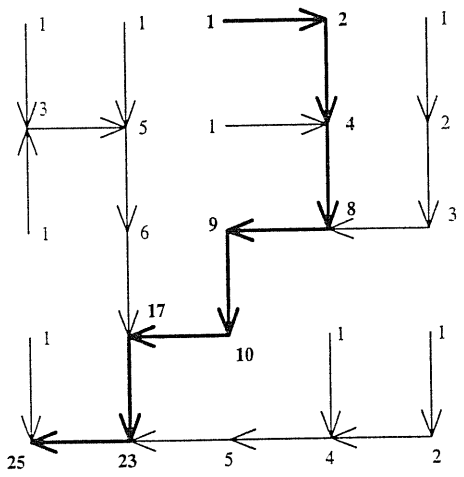

Figure 1.4: A small map of drainage directions with the values of drained area displayed.

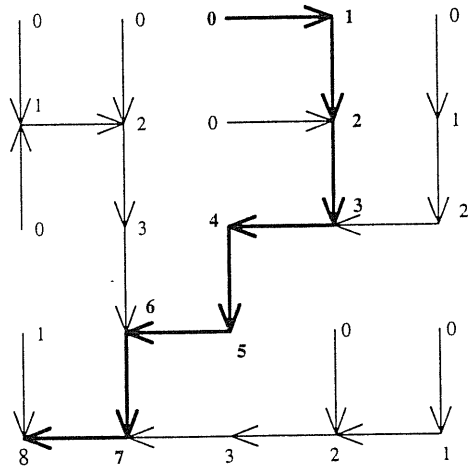

Figure 1.5: A small map of drainage directions with the values of main stream length displayed.

Note that if we choose as site i the outlet the drained area and the main stream length will be respectively the total area of the basin and the longest stream in there.

1.3 Experimental evidences

The importance of DEM can be easily understood. They made available an enormous amount of data recovered from basins in the most different environmental conditions and of the most different sizes. Thanks to them has been possible to extensively test all the known empirical laws and new ones have been discovered. Moreover they furnished a complete and detailed description of the three dimensional structure of hillslope linking it to the bidimensional structure of the channel network. All these informations have been lacking since a long time.

One of the oldest and best known empirical law regarding river network is the Hack law [9]. In 1957 Hack reported the results of his studies made on some basins of Shenandoah Valley and in adjacent mountains in Virginia showing that the longest stream and the drained area of a basin are related by a simple power law relation, namely

$$l \sim a^h \tag{1.3}$$

where the accepted value for h is $h \sim 0.57 - 0.6$. After that, by mean of DEM, Hack's relation has been tested recovering data from a big number of basins. The same test has been performed also within single basins, considering each point i as the outlet of the sub-basin made of all the sites upstream with respect to i. Results of some of these experiments are shown in figure (1.6).

Two are the main suggestions coming from Hack's law: from one side the quite surprising universality of the exponent h that seem to be the same for all basin considered; the second that some sort of fractal behavior should be considered to explain the Hack's law. The same Hack and then Mandelbrot [10] noted that , if geometrical similarity is to be preserved as a drainage basin increase in size the exponent linking l and a should be $h = 0.5$

Both these two issues have been confirmed by further analysis of the geometrical features of channel networks. In order to characterize the geometry of channel networks, geologists measured the distribution of drained area $p(a)$ and of the main stream lengths $\pi(l)$. They are respectively the fraction of sites in the lattice in which the drained area is equal to a and the fraction of sites in which the mainstream length is equal to l. Results of these measure for the Raccoon river (USA), together with its map of drainage directions are shown in figure (1.7).

Two important features emerge [11, 12, 13]: both $p(a)$ and $\pi(l)$ are characterized by a very

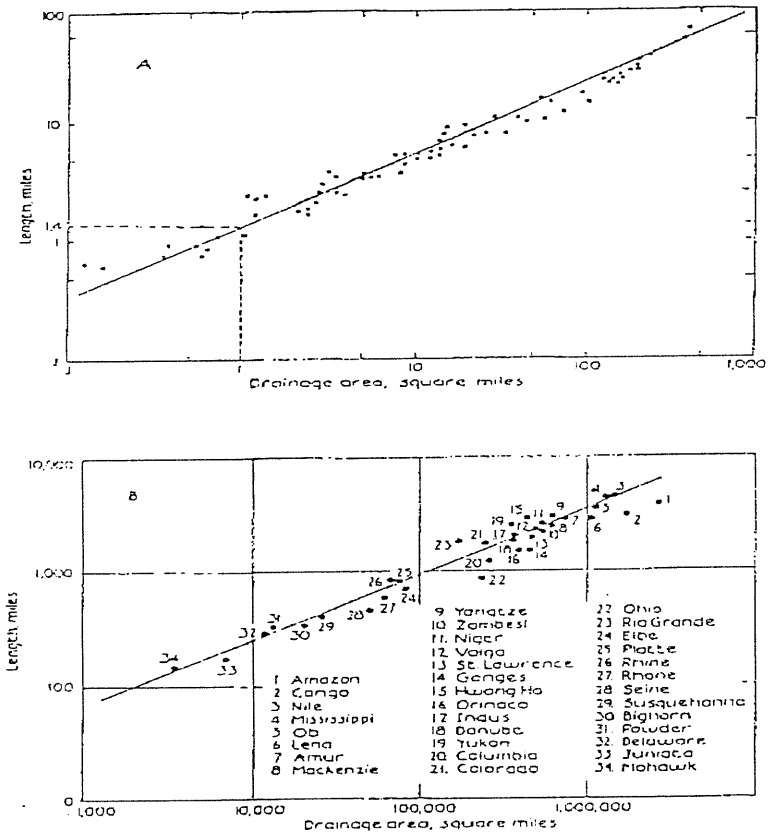

Figure 1.6: B: main stream length against area for different basins. A: main stream length against drained area within the same basin

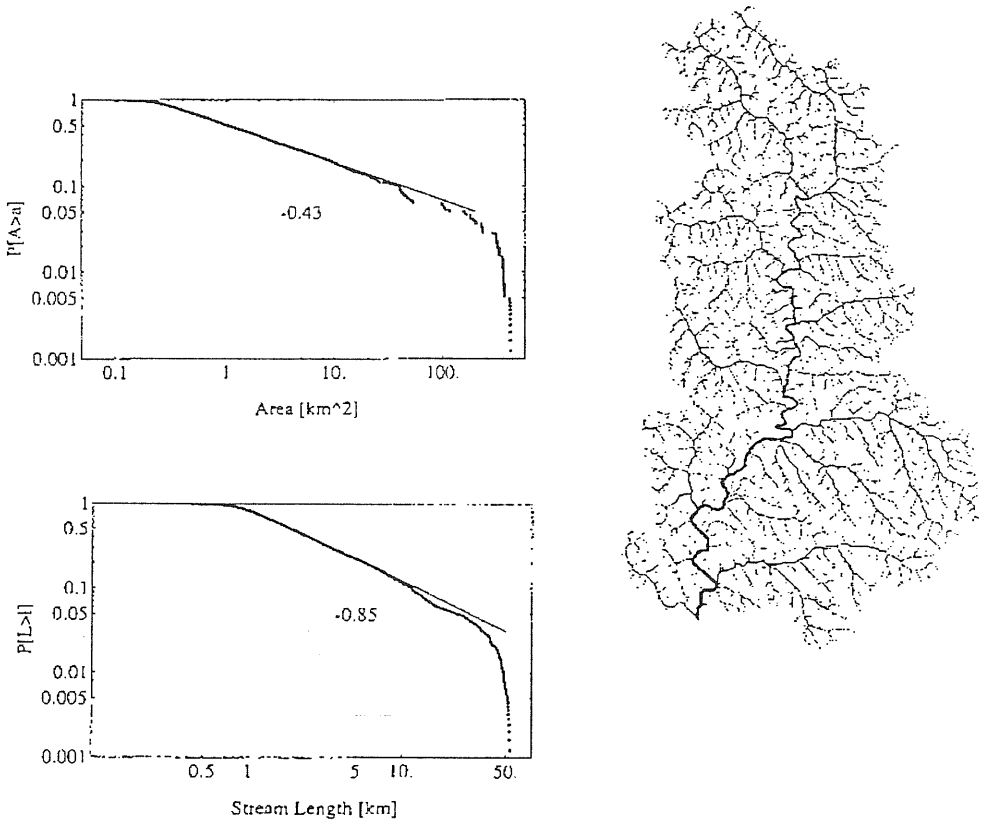

Figure 1.7: The distribution $P(A > a)$ and $\Pi(L > l)$ together with the map of drainage directions for the river Raccoon (USA)

well defined power law tails over several order of magnitude, i.e.

$$\begin{aligned} p(a) &\sim a^{-\tau} \\ \pi(l) &\sim l^{-\psi}. \end{aligned} \tag{1.4}$$

To some extent this experimental evidence could be expected. Power law behavior of $p(a)$ and of $\pi(l)$ is the direct consequence of the self-similar character of channel network, that , at least qualitatively, could be guessed just by looking at the map of drainage directions obtained from DEM. We will see in the next Chapter that in effect distribution of drained area and of main stream length for tree-like structures have often power law behavior.

Surprisingly both τ and ψ result to have almost the same values, irrespectively from the peculiar characteristics of the basin they refer to. The accepted experimental values for τ and ψ are

$$\begin{aligned} \tau &\sim 1.40 - 1.45 \\ \psi &\sim 1.80 - 1.85. \end{aligned} \tag{1.5}$$

This experimental evidence of universality gave strong support to the idea that a model attempting to reproduce the geometrical features of river basin could neglect lot of environmental 'details'.

We have to mention one more well established empirical evidence [4], which goes under the name of slope-discharge relation and states that, see figure (1.8), if water is flowing from site i to site j, the drop in elevation between site i and site j is proportional to a power of the quantity of water Q_i flowing in i :

$$\nabla h(i) \doteq h_i - h_j \sim k_i Q_i^{\gamma-1} \tag{1.6}$$

where j is the site immediately downstream of i, k_i a constant of proportionality depending on the site and the experimental value of γ is around 0.5.

Note that Q_i can be written as

$$Q_i = \sum_{j \in up(i)} r_j \tag{1.7}$$

where r_j is the precipitation at site j and where the sum runs over all sites upstream respect to i. If we assume uniform unitary rainfall (i.e. $r_i = 1 \forall i$) then

$$Q_i = A_i \tag{1.8}$$

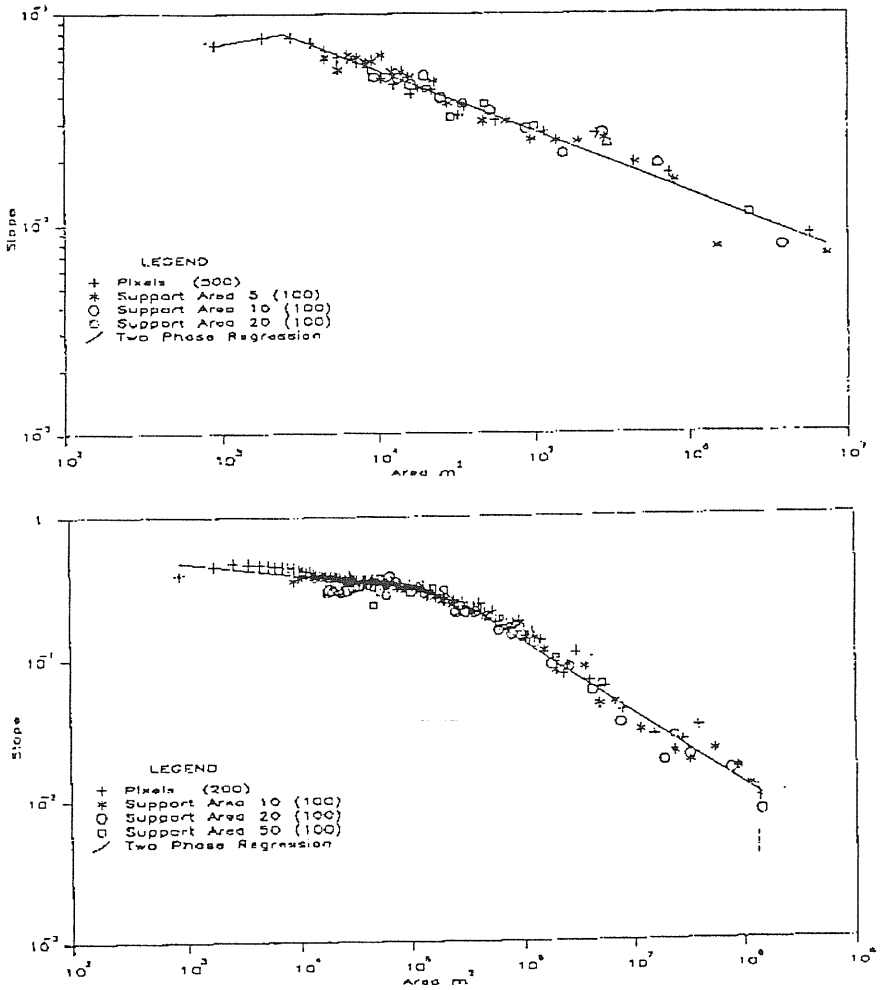

Figure 1.8: Results of some experimental tests of the slope-discharge relation

The slope-discharge relation is a result of great importance because, in a sense, bridges the structure of channel network to the hillslope.

Assuming the validity of the slope-discharge relation, the distributions of the drop in elevation along the stream can be straightforward computed from the distribution of the drained area. Moreover, if the map of drainage directions is given, the elevation field can be exactly reconstructed using (1.6). It turns out that a complete description of the river basin can be given only in terms of the bidimensional features of the channel network. This is the reason why the distributions of drained area and of mainstream length play a central role for the description of river basin morphology.

In this work we will discuss the Optimal Channel Network (OCN) model [14, 15]

It is based on the idea that drainage network can be obtained by a principle of optimality. In the specific case of river basins it is assumed that real channel networks minimize the rate of energy dissipation.

The energy dissipated by an arbitrary channel network can be computed once the map of drainage directions is given. Indeed, using the slope-discharge law, it can be expressed in terms of the only drained areas and the OCN will be that spanning tree (i.e. map of drainage directions) which realize the minimum of the functional 'dissipated energy'.

The energy dissipated by a channel network can be evaluated as follow. If one assume that the velocity of water is the same in all the points of the basin, it turns out that all the potential energy of water incoming in the system by precipitation is dissipated through friction and erosion because there is no gain in kinetic energy. The energy E_i dissipated in link i is given by the mass of water flowing in there times the drop in elevation along the stream

$$E_i = Q_i \nabla h_i. \tag{1.9}$$

If one further assume homogeneous precipitation and the slope-discharge relation finds for the total dissipated energy E

$$E = \sum_i k_i A_i^{\gamma} \tag{1.10}$$

where γ is the parameter in the slope-discharge relation and its value is fixed by experiments to be around 0.5. To overcome uncertainty due to experimental error we will consider γ as a parameter and $\gamma \in [0, 1]$

1.4 Plan of the work

In the next Chapter we will introduce [16] a finite size scaling for the distribution of drained area and of mainstream length. In this framework the phenomenological behavior observed for these distributions find a natural and simple explanation.

Assuming the finite size scaling behavior and by mean of quite simple arguments dictated by the three-like structure of channel network and by some of the experimental evidences previously discussed, we will work out two relations between the scaling exponent introduced. The distributions computed by experimental data are found to be fitted quite well in the finite size scaling form proposed and the measured exponents are in accord with scaling relations.

In Section 2.2 we briefly discuss some early models of rivers. These models have the common feature to deal exclusively with the bidimensional drainage structure of the river network. In these models different rules are given, based on randomness or deterministic, to generate spanning tree over a lattice. Despite of their simplicity all these models capture some features of real river networks, namely, they all give place to self similar structure characterized by power law distributions of drained area and of mainstream length. In all the case examined we will find the finite size scaling to be correct and the exponents verify our scaling relations.

In the third Chapter we will describe the Optimal channel Network (OCN) introduced some years ago by Rinaldo and Iturbe.

This model is based on very simple rules and depends on one only parameter γ.

For different values of exponent γ OCN model shows a lot of interesting features, recovering for the extremal values classes of spanning trees already studied.

We will work out exactly the scaling behavior of OCN for a set of values of the parameter which includes the extremal cases and the physical one. In the physical case we find a sort of mean field behavior characterized by exponents substantially different from the experimental ones. Thus we have addressed the study of various universality classes along various directions.

What happens if disorder is added to the model ? There are two cases: the first simulating randomness in the precipitation and the second with inhomogeneities in the soil properties. Also in this two cases it is possible to find the exact scaling behavior. In the latter case we mapped the problem in the well studied problem of a polymer in a random environment with weak disorder.

At the end OCN will give three different universality classes, i.e different set of values for the exponent of the drained area and of main stream length, all in accord with the scaling

relations but none of them in agreement with real data.

In the last Chapter we discuss the numerical simulations we performed for OCN model and the possibility to face the problem with a 'termodynamical' approach.

The search of optimal configuration has been made with different algorithms. With a very slow and accurate annealing we obtain results which are in perfect agreement with our exact predictions of Chapter three. Quite surprisingly, if a less accurate algorithm is used we recover a set of configurations substantially different from the ones above, but nevertheless with a their own well defined identity characterized by exponents satisfying the scaling relations and, within the statistical error, coincide with the experimental data. Is it a pure coincidence, or there is some deep reason for the fact that configurations found with a less clever algorithm are so close to the one which occurs in Nature ? This is the question we will try to answer in conclusion and that arose the concept of Feasible Optimality..

2 Finite size scaling, scaling relations and examples

A river basin is a complex system made of two strongly interrelated elements: the channel network and the underlying structure of hillslope.

The channel network can be described by a set of drainage directions, i.e. by an oriented spanning tree over a lattice.

Experimentally the sets of drainage directions can be constructed with great accuracy by mean of DEM. They exhibit a very well defined self-similar structure. This experimental evidence is confirmed by looking at the distributions of drained area and of main stream length which are extracted by the maps of drainage directions and which exhibit a power laws behavior over several decades.

Understanding the scaling behavior of these quantities is of great importance. The statistical properties of the whole system (hillslope + channel network) can be in fact computed using the slope discharge relation once the set of drainage directions is known.

Self-similarity [10] is the property of those object which show the same features, at least in statistical sense, independently by the scale at which you are looking at. In other words if a small part of a self similar object is enlarged by an arbitrary factor it will appear to be the same as the whole object, no matter how large is the scale factor chosen. This property reflects in power law distribution for the geometrical quantity which describe the object.

In real systems such a strong similarity between the whole and the part cannot be expected if the part has been magnificated by a too large factor. This yields to corrections at the power law behavior taking into account the finite size of the system. To consider such corrections demonstrates very fruitful in a lot of problems where physical self similarity is involved [17, 18, 19]. This happens for example in ferromagnetic systems very close to the critical point, so close that the correlation length became comparable with the linear size of the entire system.

Finite size corrections to scaling have been considered for the distributions of drained area

and of main stream length of river basin by [16]. In this framework phenomenological observations find a natural and simple explanation.

In the first Section we introduce the finite size scaling and derive relations between scaling exponents. Using these relations the behavior of river basin under scale transformations can be described by only two independent exponents which reduce to one if we further assume that fractality of the single stream and self similarity of the plan shape of the basin cannot coexist.

In Section two and three we discuss two early models of river network, proposed about thirty years ago respectively by Leopold and Langbein [1] and Scheidegger [20]. Both these model deal exclusively with the two dimensional structure of channel networks. Using simple rules they generate different classes of random spanning trees.

Both these models exhibit self similarity and are characterized by power law behavior of distributions of drained area and of main stream length.

The τ exponent for the distribution of drained areas in the Scheiddeger model has been exactly calculated by Takayasu et al. [21, 22] by mapping it on a model of random aggregation. We show that the distribution of mainstream length can be calculated in a similar way and that the exponents τ and ψ are in agreement with scaling relations derived in Section 2

In Section four we analyze the Peano basin. It is a deterministic fractal introduced [10, 23] to study some geometrical features of stream aggregation. We calculate [24] the exact scaling behavior and also in this case scaling relations turns out to be verified, furthermore an exact renormalization group is introduced.

In the last Section we report results about geometrical properties of a random spanning tree. The set of all spanning trees over a given lattice emerge in several problems of Statistical Mechanics, but we will think at them as the most general structure that can arise from a DEM.

The scaling exponents are known exactly from the work of Coniglio [25] and Manna et al. [26] and they are in accord with scaling relations.

It should be stressed that the analysis of all these models is not purely academic. Lot of ideas about scaling relations and OCN have been developed and tested considering these models. The knowledge of the scaling behavior of Peano basin, in particular, will be a key result for the analysis of OCN model, as we will see in the next Chapter.

Moreover, in the context of OCN Scheiddeger trees and the set of all spanning trees realize the minimum of energy expenditure for particular values of the parameter γ from which the dissipated energy depends on.

2.1 Scaling Relations

For a given tree, one may consider the probability distribution of the following quantities: for a lattice of given linear size L we will call $p(a, L)$ the probability density of accumulated areas a and $\pi(l, L)$ the probability density of the upstream lengths l. These represent the fraction of sites with area a or stream length l respectively. We will also consider the integrated probability distributions $P(a, L)$, the probability to find an accumulated area bigger then a and $\Pi(l, L)$, i.e. the probability to have a site with an upstream length bigger than l.

Both these probability distributions, here defined in the simple case of the lattice model, were originally introduced to describe real rivers and experimentally found to scale as power laws leading to the formulation of a finite size scaling ansatz

$$p(a, L) = a^{-\tau} f\left(\frac{a}{a_C}\right), \tag{2.1}$$

$$\pi(l, L) = l^{-\psi} g\left(\frac{l}{l_C}\right), \tag{2.2}$$

where $f(x)$ and $g(x)$ are scaling functions accounting for finite size effects and a_C and l_C are the characteristic area and length respectively. The functions $f(x)$ and $g(x)$ are postulated to have the following properties: when $x \to \infty$ they go to zero sufficiently fast to ensure normalization; when $x \to 0$ they tend to a constant, to yield simple power law behavior of the probability distributions in the large size limit. This also implies that τ and ψ are bigger than one.

The characteristic area and length are postulated to scale as

$$a_C \sim L^{\Phi}, \tag{2.3}$$

$$l_C \sim L^{d_l}. \tag{2.4}$$

In river basins, anisotropies are always present due to a non-zero average slope of the landscape and the presence of gravity. Thus, one has to distinguish between a typical longitudinal length L and a typical perpendicular one $L_\perp$ (these two length are measured along the two principal axis of inertia), which scale as

$$L_\perp = L^H, \tag{2.5}$$

giving $a_C \sim L^{1+H}$, i.e. $\Phi = 1 + H$. H is known as the Hurst exponent and of course $0 \leq H \leq 1$. In what follow, for the sake of simplicity, we consider basins of square shape; the above relations then, refers to dimension of a generic sub-basin inside the bigger one, whose dimensions are fixed from outside.

The Φ exponent thus corresponds to $\Phi = 1 + H$. The d_l exponent, characterizing the typical length, can be assumed to be the fractal dimension of a stream (for fractal river networks, each rivulet going from any site to the outlet is a fractal with the same fractal dimension) , and is such that $1 \leq d_l \leq 1 + H$. The bounds correspond to a straight line and a space-filling behavior. For self-affine river basins we expect $d_l = 1$ and $H < 1$, whereas, when $H = 1$ then $d_l > 1$ in the self-similar case.

For the same quantities, the integrated probability distributions can be analogously written:

$$P(a, L) = a^{1-\tau} F\left(\frac{a}{L^{1+H}}\right), \tag{2.6}$$

$$\Pi(l, L) = l^{1-\psi} G\left(\frac{l}{L^{d_l}}\right), \tag{2.7}$$

which follow from (2.1) and (2.2) with

$$F(x) = x^{\tau-1} \int_x^{+\infty} dy\ y^{-\tau} f(y), \tag{2.8}$$

$$G(x) = x^{\psi-1} \int_x^{+\infty} dy\ y^{-\psi} g(y), \tag{2.9}$$

where sums over variable y have been replaced by integrals in large L limit.

From the above definitions and the properties of f it easily follows that

$$\langle a^n \rangle \sim L^{(1+H)(n-\tau+1)}, \tag{2.10}$$

for any $n > \tau - 1$, while $\langle a^n \rangle \sim const.$ if $n < \tau - 1$. Note that both a and l have a lower cutoff which is one.

This equation, evaluated for $n = 1$ gives for the average area,

$$\langle a \rangle \sim L^{(1+H)(2-\tau)}. \tag{2.11}$$

The mean accumulated area $\langle a \rangle$ can be easily shown to be equal to the distance from a site to the outlet, averaged over all sites. In effect, in the sum over all the downstreams (the rivulets going from each site to the outlet), the number of times each bond (of unit length)

appears exactly equals the accumulated area of the associated site. Thus summing over all A_i is equivalent to a sum over all the downstream lengths:

$$\langle a \rangle = \langle l_{downstream} \rangle \,. \tag{2.12}$$

$\langle l_{downstream} \rangle$ can be evaluated replacing in the sum the distance of each point from the outlet measured along the stream with the corresponding Euclidean distance $d(x)$ to the power d_l:

$$\langle l_{downstream} \rangle = \frac{1}{L^2} \sum_x l_{downstream}(x) = \frac{1}{L^2} \sum_x d(x)^{d_l} \sim L^{d_l} \tag{2.13}$$

This fact is general and the argument we used does not need the knowledge of the downstream length distribution. This distribution however can be explicitly derived at least in the case of *directed* networks. We call *directed* those networks such that each oriented link has positive projection along the diagonal oriented towards the outlet.

The reason to introduce this class of networks is that river basins often have a *quasi-directed* character, due to the fact that they are typically grown on a slope which gives a preferred direction to the flow. Moreover directed trees are much more simple to handle analytically than "undirected" ones.

For such trees consider the set of $2L$ diagonals orthogonal to the one passing through the outlet: the downstream length is the same for all the points on the same diagonal. Thus the number of points at a given distance to the outlet can be easily seen to be:

$$\text{number of point at distance } l = \begin{cases} l+1 & l = 1,..L \\ 2L+1-l & l = L+1,..2L \end{cases} \tag{2.14}$$

thus the probability density for the downstream lengths has the form of a power law with exponent -1 times a scaling function of the argument l/L:

$$\pi_{downstream}(l, L) = l^{-1} f_{downstream}\left(\frac{l}{L}\right) \tag{2.15}$$

with

$$f_{downstream}(x) = \min(x^2, 2x - x^2) \quad 0 \le x \le 2 \tag{2.16}$$

The first moment of this distribution again gives eq. (2.13) with $d_l = 1$ which is the expected result for the fractal dimension of a directed tree. This result, together with (2.13) suggest that downstream length distribution might have the scaling form:

$$\pi_{downstream}(l, L) = l^{-1} f_{downstream}\left(\frac{l}{L^{d_l}}\right) \tag{2.17}$$

for the general case.

Equations (2.12) and (2.13) lead to the following expression for the average area:

$$\langle a \rangle \sim L^{d_l} . \tag{2.18}$$

From eq.(2.18) and eq.(2.11) we get the scaling relation

$$1 + H = \frac{d_l}{(2 - \tau)} . \tag{2.19}$$

A well known hydrological law, Hack's law [9], relates the length of the longest stream l in the drained area to the drained area a of the basin:

$$l \sim a^h . \tag{2.20}$$

The accepted value of h is $h = 0.57 \pm 0.06$ [27, 28, 29], whose difference from the Euclidean value 0.5 lead to the first suggestion of the fractal nature of rivers [10].

From equations (2.3) and (2.4) it follows that

$$h = \frac{d_l}{1 + H} . \tag{2.21}$$

Together with π and p one can define the conditional probability $\tilde{\pi}(l \mid a)$ of finding a main stream with length l in a basin with accumulated area a. The simplest scenario is that (2.20) still holds and [16, 30] $\tilde{\pi}(l \mid a)$ is a sharply peaked function of l with respect to a, i.e. there exists a well-defined constraint between lengths and areas,

$$\tilde{\pi}(l \mid a) = \delta(l - a^h) , \tag{2.22}$$

or more generally [31],

$$\tilde{\pi}(l \mid a) = l^{-1} \tilde{g}\left(\frac{l}{a^h}\right) . \tag{2.23}$$

For the probability density π, p and $\tilde{\pi}$ the following consistency equation must hold:

$$\pi(l, L) = \int_1^{L^{(1+H)}} da \; \tilde{\pi}(l \mid a) p(a, L) \tag{2.24}$$

that gives, in the large L limit

$$(\psi - 1)d_l = (\tau - 1)(1 + H) \tag{2.25}$$

relating the exponents in the distribution of lengths and in the distribution of accumulated areas.

The scaling relations (2.19) and (2.25) can be expressed in a simpler form, observing that both τ and ψ depend on d_l and H only in the combination $\frac{d_l}{(1+H)} = h$, where h is the parameter appearing in Hack's law (2.20). Thus

$$\tau = 2 - h, \tag{2.26}$$

$$\psi = \frac{1}{h}. \tag{2.27}$$

The exponents characterizing the distributions of accumulated areas and upstream length are thus related by the simple expression:

$$\tau = 2 - \frac{1}{\psi}. \tag{2.28}$$

Since $h \geq \frac{1}{2}$, then $\tau \leq \frac{3}{2}$.

2.2 An early model of river network

One of the first attempt to reproduce statistical feature of a channel network by mean of a bidimensional model is due to Leopold and Langbein [1].

The model they proposed is very simple, nevertheless it is able to capture some significative aspects of the geometry of real rivers. The idea on which it is based is that each single point can drain to the outlet following a random walk since a previously generated path is met.

Inspired by the work of Leopold and Langbein, twenty years later, Meakin, Feder and Jøssang considered a very similar model and studied it extensively. We report about the latter work [32].

Meakin et al. considered a square lattice of size L. The network of channel was constructed as follow: from a random chosen site a Self Avoiding Walk (SAW) is started and prosecuted until it reach the border of the lattice. The procedure is then iterated extracting a new site, starting a SAW from there which ends when a border site or a previously generated path is reached. When each point results to be connected to a border site (i.e. an outlet) iteration is stopped.

Two different rules are used to avoid self -intersections of a walker with its own steps.

In the first version, model SAWa, at each time step the walker consider its environment and choose at random, if possible, a move that does not give place to self-intersections. If it is not possible the walker goes one step back and a new move is selected at random but neglecting the possibility to go back in the trapped configuration where he is coming from. The procedure is iterated until the walker meet a border or a path generated by a previous walker.

In the second version, model SAWb, when the model get in a trapped configuration a new attempt is made to generate a SAW from the same starting site.

Once the network has been constructed with one of these two rules, they measure the drained area and the main stream length for the sites on the border of the lattice (the outlets). They found these two quantities related by a power law, with different exponent in the two cases, but both quite close to the exponent measured by Hack on real basins:

$$l_a \sim A^{h_a} \quad h_a \sim 0.6 \pm 0.05 \tag{2.29}$$

$$l_b \sim A^{h_b} \quad h_b \sim 0.62 \pm 0.01 \tag{2.30}$$

Also the distribution of drained area for border site has been measured, i.e. the fraction $p(A, L)$ of sites on the border with an accumulated area equal to A. They state that this distribution is well fitted in the form:

$$p(a, L) = a^{-\tau_\delta} f_\delta(\frac{a}{\Phi_\delta}) \tag{2.31}$$

here the δ indicates that only sites on the border have been considered. In the two models they measured:

$$\tau_\delta = 1.390 \pm 0.005, \ \Phi_\delta = 1.80 \tag{2.32}$$

for model SAWa and

$$\tau_\delta = 1.373 \pm 0.005, \ \Phi_\delta = 1.80 \tag{2.33}$$

for model SAWb.

Note that the distribution of drained area considered by Meakin is similar to (2.1), but only sites lying on the border are considered here. In this case a relation analogous to (2.19)

between τ and Φ can be easily derived observing that the sum of all drained areas on the border is exactly equal to the total area $\mathcal{A} = L^2$ covered by the basin. Then:

$$\mathcal{A} = L^2 = L \int a^{-\tau_\delta} f_\delta(\frac{a}{\Phi_\delta})da. \tag{2.34}$$

which leads to:

$$\Phi_\delta(2 - \tau_\delta) = 1. \tag{2.35}$$

2.3 The Scheiddeger Model

In the same spirit of Leopold and Langbein in 1967 Scheiddeger proposed a model trying to reproduce the structure of a channel network by mean of intersecting random walks [20].

He was interested in Alpine Valleys and so he considered necessary to give a preferential direction to the random walkers in order to simulate the strong bias to the motion of water given by the high gradients in the direction of the main Valley.

His model can be described as follow: consider a triangular lattice from which all horizontal links (i.e. links parallel to the x axis) have been deleted, being y the preferred direction.

In each site with coordinate $y = \overline{y}$ drainage direction can be chosen at random going from the point to its nearest neighbor on the right or on the left with coordinate $y = \overline{y} + 1$, with equal probability.

Executing this procedure we end up with typical patterns as the one in figure (2.1).

We can consider the distribution of drained area and of main stream length for points with $y = L$ also in this model. In figure (2.1) the drained area A_i and the main stream length l_i of point i are respectively the number of sites inside the dashed lines and the length of the darker path respectively.

Both the distributions of drained area and of main stream length exhibit a power law tail and in the same notations of previous sections, a finite size scaling ansatz can be formulated:

$$p(a, L) = a^{-\tau} f\left(\frac{a}{a_C}\right), \tag{2.36}$$

$$\pi(l, L) = l^{-\psi} g\left(\frac{l}{l_C}\right). \tag{2.37}$$

Interestingly, Huber [33] has shown that Scheiddeger model is equivalent to a 1-dimensional model of random aggregation studied by Takayasu and Takayasu [22] and Takayasu et al.

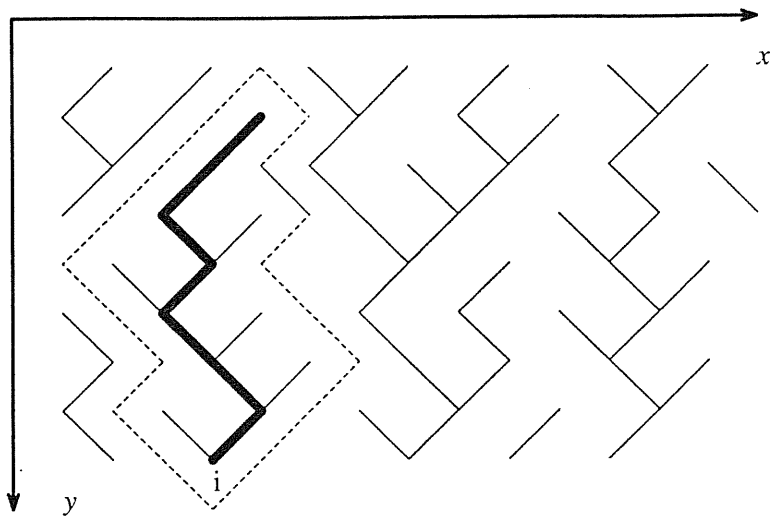

Figure 2.1: A typical pattern of Scheiddeger model. The drained area A_i (sites inside dashed lines) and the main stream l_i (bold path) for site i are displayed

[21].

This model consists of a 1-dimensional lattice on which, at time 0, there is a particle of mass $m_i = 1$ on each site i. At each time step each particle can decide with equal probability if stay where it is or if jump to the right nearest neighbor. Whenever two particles met on the same site they aggregate to give place to a particle whose mass is the sum of masses of aggregating particles. Moreover, at each time step, a particle of unitary mass is injected in each site.

The Scheiddeger and the Takayasu model can be easily seen to be equivalent representing the time evolution of Takayasu model on the same lattice used by Scheiddeger and taking the time axes parallel to the (-1,-1) direction, see figure (2.2).

The probability to have in a site a mass $m = A$ after a time $t = L$ in the aggregation model is then the same to have a drained area $a = A$ in a site with $y = L$ in Scheiddeger model.

The exponent τ of the power law tail of the distribution of the masses at time t can be calculated as follows.

Let $A_i(t)$ be the mass of the particle at site i and at time t. Then, A_i at different times are related by:

$$A_i(t+1) = A_i(t)\omega_i + A_{i-1}(t)(1-\omega_{i-1}) + 1 \tag{2.38}$$

where the $\omega_k(t)$ are random variables such that:

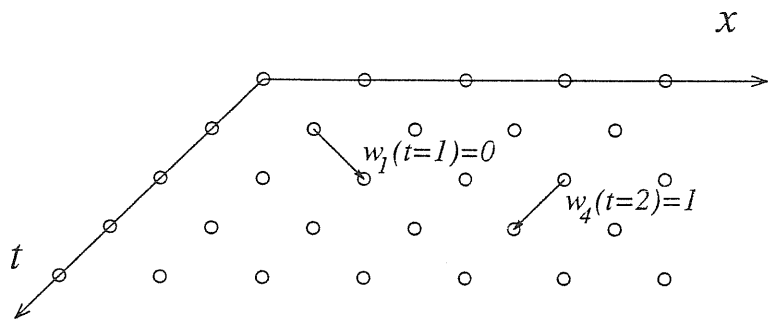

Figure 2.2: The motion of particle at site x and at time t in Takayasu model corresponds to drainage direction of at point (x,t) in Scheiddeger model

$$\omega_k(t) = \begin{cases} 1 & \text{if particle at } k \text{ stay} \\ 0 & \text{if particle at } k \text{ jump} \end{cases} \tag{2.39}$$

and, see figure (2.2),

$$\omega_k(t) = \begin{cases} 1 & \text{with probability } 1/2 \\ 0 & \text{with probability } 1/2 \end{cases} \tag{2.40}$$

We can define an r-point characteristic function for the random variable $\overline{A}_r(t) = \sum_{i=1}^{r} A_{i(t)}$:

$$\mathcal{Z}_r(s,t) = \langle e^{-s(\sum_{i=1}^{r} A_{i(t)})} \rangle_\omega \tag{2.41}$$

where the expectation value is made over all $\omega(t')$ for $t' \in [0, t-1]$. By expanding the sum in equation (2.41) and using (2.38) yields:

$$\mathcal{Z}_r(s,t+1) = \langle e^{-s(A_1(t+1)+\cdots+A_r(t+1)} \rangle_\omega = e^{-sr} \langle e^{-s(\sum_{i=1}^{r} A_i(t))} e^{-s(A_0(t+1)(1-\omega_0)} e^{-s(A_r(t+1)\omega_r} \rangle_\omega \tag{2.42}$$

taking expectations with respect to the $\omega(t)$ which are independent from $\omega(t')$ for $t' < t$ and then from $A(t)$ yields

$$\mathcal{Z}_r(s,t+1) = \frac{e^{-sr}}{4}[2\mathcal{Z}_r(s,t) + \mathcal{Z}_{r-1}(s,t) + \mathcal{Z}_{r+1}(s,t)] \tag{2.43}$$

In the limit $t \to \infty$ we can argue:

$$\lim_{t\to\infty} \mathcal{Z}_r(s,t) = \lim_{t\to\infty} \mathcal{Z}_r(s,t+1) = \mathcal{Z}_r(s). \tag{2.44}$$

equation (2.43) becomes:

$$\mathcal{Z}_{r+1}(s) + (2 - 4e^{-sr})\mathcal{Z}_r(s) + \mathcal{Z}_{r-1}(s) = 0 \tag{2.45}$$

with the initial condition:

$$\mathcal{Z}_0(s) = 1. \tag{2.46}$$

Equation (2.45) can be rewritten as:

$$\frac{\mathcal{Z}_{r-1}(s)}{\mathcal{Z}_r(s)} = (4e^{-sr} - 2) - \frac{1}{\frac{\mathcal{Z}_r(s)}{\mathcal{Z}_{r+1}(s)}} \tag{2.47}$$

and using boundary condition (2.46)

$$\frac{1}{\mathcal{Z}_1(s)} = (4e^{-sr} - 2) - \frac{1}{\frac{\mathcal{Z}_1(s)}{\mathcal{Z}_2(s)}} \tag{2.48}$$

Equation (2.48) and equation (2.47) used recursively lead to the following expression:

$$\mathcal{Z}_1(s) = \frac{1}{4e^s - 2 - \frac{1}{4e^{2s} - 2 - \frac{1}{4e^{3s} - 2 - \cdots}}} \tag{2.49}$$

If we are interested in the behavior of the distribution function for $a \to \infty$ we can expand the characteristic function around $s = 0$. Doing that term by term

$$\mathcal{Z}_1(s) = \frac{1}{2 + 4s - \frac{1}{2 + 8s - \frac{1}{2 + 12s - \cdots}}} \tag{2.50}$$

This gives, using a similar expansion which holds for Bessel functions

$$\mathcal{Z}_1(s) = 1 + cs^{1/3} + o(s) \tag{2.51}$$

From the behavior of the characteristic function $\mathcal{Z}_1(s)$ for small s we can derive inverting Laplace Transform the behavior of distribution of mass $p(a, L = \infty)$ for large a giving:

$$p(a, L = \infty) \sim a^{-\frac{4}{3}} \tag{2.52}$$

i.e. $\tau = 4/3$. Using an argument analogous to the one which lead to (2.34), that also in this case hold exactly, yields

$$\Phi = \frac{1}{2 - \tau} = \frac{3}{2} \tag{2.53}$$

With a similar calculation we can derive the exponent ψ of the distribution of main stream length. Note that the main stream length in a point in the Scheiddeger model corresponds in Takayasu model to the age of oldest particle who takes part in a aggregate particle, see figure (2.1). Following the previous calculation we can define a random variable $l_{[1,r]}(t)$ as the age of the oldest particle which is aggregated to one of the particles which are at sites $i = 1, 2, \cdots, r$ at time t. These variables are related to the analogous variables at the previous time step by

$$l_{[1,r]}(t+1) = \begin{cases} l_{[0,r]}(t)+1 & \text{if } \omega_0(t)=0 \text{ and } \omega_r(t)=1 \\ l_{[0,r-1]}(t)+1 & \text{if } \omega_0(t)=0 \text{ and } \omega_r(t)=0 \\ l_{[1,r]}(t)+1 & \text{if } \omega_0(t)=1 \text{ and } \omega_r(t)=1 \\ l_{[1,r-1]}(t)+1 & \text{if } \omega_0(t)=1 \text{ and } \omega_r(t)=0 \end{cases} \tag{2.54}$$

and, as before

$$\omega_k(t) = \begin{cases} 1 & \text{if particle at k stay} \\ 0 & \text{if particle at k jump} \end{cases} \tag{2.55}$$

and

$$\omega_k(t) = \begin{cases} 1 & \text{with probability } 1/2 \\ 0 & \text{with probability } 1/2 \end{cases} \tag{2.56}$$

Analogously at the case of masses we can consider an $r-$points characteristic function

$$\mathcal{L}_r(s,t) = \langle e^{-sl_{[1,r]}(t)} \rangle_\omega \tag{2.57}$$

where the expectation is made over all $\omega(t')$ for $t' \in [0, t-1]$. By using equation (2.54) and the fact that variables $l_{[.,.]}$ involving the same number of sites are equally distributed due to the translational invariance we find

$$\mathcal{L}_r(s,t+1) = \frac{e^{-s}}{4}(\mathcal{L}_{r+1}(s,t) + 2\mathcal{L}_r(s,t) + \mathcal{L}_{r-1}(s,t)). \tag{2.58}$$

If we suppose that the limit $t \to \infty$ exists,

$$\lim_{t\to\infty} \mathcal{L}_r(s,t) = \lim_{t\to\infty} \mathcal{L}_r(s,t+1) = \mathcal{L}_r(s) \tag{2.59}$$

equation (2.58) becomes

$$\mathcal{L}_{r+1}(s) + (2 - 4e^s)\mathcal{L}_r(s) + \mathcal{L}_{r-1}(s). \tag{2.60}$$

The initial condition will be

$$\mathcal{L}_0(s) = 1 \tag{2.61}$$

Equation (2.60) can be rewritten as

$$\frac{\mathcal{L}_{r-1}(s)}{\mathcal{L}_r(s)} = 4e^s - 2 - \frac{1}{\frac{\mathcal{L}_r(s)}{\mathcal{L}_{r+1}(s)}}. \tag{2.62}$$

and using boundary condition (2.61) we have

$$\frac{1}{\mathcal{L}_1(s)} = 4e^s - 2 - \frac{1}{\frac{\mathcal{L}_1(s)}{\mathcal{L}_2(s)}}. \tag{2.63}$$

Again, using equation (2.63) and formula (2.62) recursively we obtain the following continued fraction

$$\mathcal{L}_1(s) = \cfrac{1}{4e^s - 2 - \cfrac{1}{4e^s - 2 - \cfrac{1}{4e^s - 2 - \cdots}}} \tag{2.64}$$

In this case the continued fraction (2.64) can be explicitly calculated leading to

$$\mathcal{L}_1(s) = 1 + 2e^s(1 - \sqrt{1 - e^{-s}}) \tag{2.65}$$

and expanding around $s = 0$

$$\mathcal{L}_1(s) = 1 + 2s^{\frac{1}{2}} + o(s). \tag{2.66}$$

Inverting the Laplace transform yields

$$\pi(l, L = \infty) \sim l^{-\frac{3}{2}}, \tag{2.67}$$

i.e. $\psi = 3/2$.

Resuming the exponents of area and length distributions for the Scheiddeger model can be computed considering an equivalent model of mass aggregation and they relate according the scaling relation (2.19) and (2.25). They are:

$$\tau = 4/3, \quad \Phi = 3/2, \quad \psi = 3/2, \quad d_l = 1 \tag{2.68}$$

Also a mean field version of this model has been considered and solved by Takayasu. It consists as before of a 1−dimensional lattice of N sites, but now particles at each time step can stay or jump with equal probability in any site. Rules of aggregation and of injection remain the same of the previous case. In this case he finds:

$$\tau = 3/2, \quad \Phi = 2, \quad \psi = 2, \quad d_l = 1 \tag{2.69}$$

Once again relations (2.19) and (2.25) holds.

2.4 The Peano Basin

Peano basin [10, 23, 24] is a deterministic space filling fractal with a tree like structure with some resemblance with that of real rivers.

Peano basin is obtained as follows. At step 0 it is an oriented link. Step 1 is obtained by replacing such link with four new links: two resulting from the subdivision in half of the old link and preserving its orientation, other two having a common extreme in the middle point of the old link and both oriented toward it (see figure (2.3)).

The basin at each successive step, is obtained iterating the construction, i.e. replacing each link with four new oriented links in the same way. After T steps the fractal has $N_T = 4^T$ points (excluding the outlet) and it can be mapped on square lattice of size $L = 2^T$ with bonds connecting first and second neighbors to form a spanning tree.

We can associate to each site i of a T step Peano basin an area $A_i(T)$ defined as in (1.1). Let $\mathcal{V}_T$ denote the set of distinct values assumed by the variables $\{A_j\}$ at step T. How can be easily checked by induction, $\mathcal{V}_T$ contains $\mathcal{V}_{T-1}$ and 2^{T-1} new distinct values, appearing for the first time. Thus $\mathcal{V}_T$ contains in all 2^T distinct numbers. Let us call $\mathcal{A} \doteq \bigcup_{T=0}^{\infty} \mathcal{V}_T$ and a_n the increasing sequence of numbers in $\mathcal{A}$ (the distinct values assumed by variables A_j iterating the construction). For such sequence, we found the following rule:

$$a_n = 3\,(\sum_k c_k(n) 4^k) + 1 \qquad n = 0, 1, \ldots \tag{2.70}$$

where the $c_k(n)$ are the coefficients of the binary expansion of n:

$$n = \sum_k c_k(n) 2^k \,. \tag{2.71}$$

Let M_n^T be the number of sites i at step T whose area A_i assume a given admissible value a_n. From the construction shown in figure (2.4) one can deduce that the following recursive

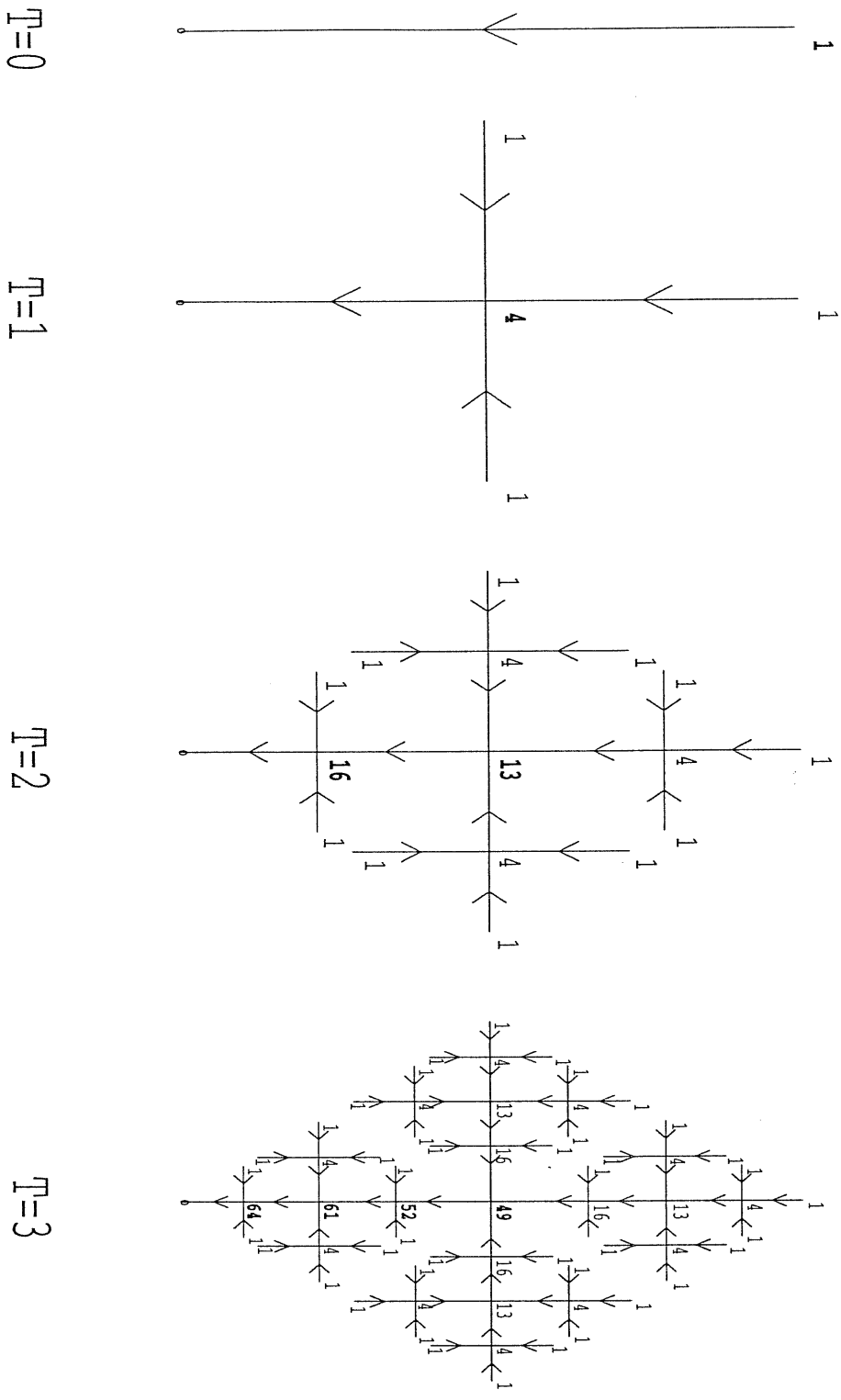

Figure 2.3: The Peano basin at iteration step $T = 0$, $T = 1$, $T = 2$, $T = 3$, with the cumulated area displayed.

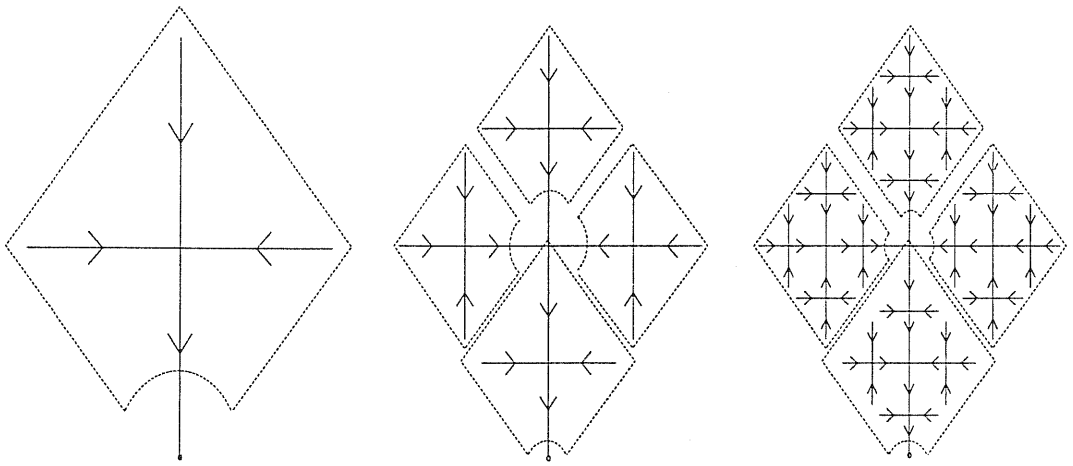

Figure 2.4: With this construction the recursive relation can be easily understood. Peano basin at time step $T+1$ is showed in terms of the one at time step T.

relation holds:

$$\begin{cases} M_n^T = 4 \cdot M_n^{T-1} - 1 & T > t(a_n) \\ M_n^T = 1 & T = t(a_n) \\ M_n^T = 0 & T < t(a_n) \end{cases} \tag{2.72}$$

where $t(a_n)$ denotes the a_n "borning time", i.e. the first step in which an area with value a_n appears.

This is easily seen to be given by

$$t(a_n) = \begin{cases} 0 & n = 0 \\ 1 + [\log_2(n)] & n > 0 \end{cases} \tag{2.73}$$

where $[\,\cdot\,]$ is the integer part.

Solving (2.72) one gets

$$M_n^T = \left\{ \begin{array}{ll} 0\,, & T < t(a_n) \\ \frac{2}{3}4^{T-t(a_n)} + \frac{1}{3}\,, & T \geq t(a_n) \end{array} \right\} \tag{2.74}$$

and thus all the a_n's "born" at the same time step have the same probability

$$p_T(a_n) \doteq p(a_n, L{=}2^T) = M_n^T / N_T \tag{2.75}$$

Then the integrated distribution of areas $P(A_i > a_n, L{=}2^T)$ assume a very simple expression for the a_n of the form 4^t (one can easily check from (2.70) that $a_{2^t-1} = 4^t$), and is given by eq. (2.6)

$$P(A_i > a{=}4^t\,,\, L{=}2^T) = a^{1-\tau} F\left(\frac{a}{L^\Phi}\right) \tag{2.76}$$

with

$$\tau = 3/2 \ , \ \Phi = 2 \tag{2.77}$$

and

$$F(x) = \frac{1}{3}(1-x) \quad , 0 < x < 1. \tag{2.78}$$

and $F(x) = 0$ when $x > 1$.

Equation (2.76) can be obtained observing that $P(A_i > a = 4^t \, , \, L = 2^T) = \sum_{n=2^t}^{2^T} p_T(a_n)$ depends on n only through $t(a_n)$, allowing the replacement of the sum over n with a sum over the steps s; moreover, for each step $s > 0$ there are 2^{s-1} areas with the same $t(a_n) = s$, thus

$$\begin{aligned} &P(A_i > a = 4^t \, , \, L = 2^T) = \textstyle\sum_{s=t+1}^{T} \left(\frac{2}{3} 4^{(T-s)} + \frac{1}{3} \right) \cdot \frac{2^{s-1}}{4^T} = \\ &= \tfrac{1}{3} 2^{-t} (1 - 2^{2(t-T)}) = \tfrac{1}{3} a^{-\frac{1}{2}} \left(1 - \tfrac{a}{L^2} \right), \end{aligned} \tag{2.79}$$

which yields eqs. (2.76)-(2.78). Similarly, choosing l of the form $l = 2^t$ and observing that at step T the sites with upstream length bigger or equal to 2^t are the ones in which the cumulative area exceeds 4^t, we easily find:

$$\Pi(l \geq 2^t, L = 2^T) = l^{1-\psi} G\left(\frac{l}{L^\delta} \right) \tag{2.80}$$

which is of the form (2.7) with

$$\psi = 2 \ , \ \delta = 1 \tag{2.81}$$

and

$$G(x) = \frac{1}{3}(1 - x^2) \, . \tag{2.82}$$

Scaling exponents for the Peano basin can also be obtained by a renormalization group argument. Let us consider for instance the scaling of cumulated areas.

The self-similar structure of the Peano basin suggests a natural "decimation" procedure [34]; the idea is the following: consider the equations relating areas at time step T; then, eliminate variables related to sites that are not present at time step $T-1$. This leads to a reduced equation describing the same physics on a tree scaled down by a factor 2.

For the sake of simplicity let us consider the Peano basin at the second step of iteration.

In figure (2.5) $A_n^{(2)}$ denote the variables related to sites that are present at step $T = 1$ and $B_n^{(2)}$ denote the ones that will be eliminated by decimation. The upper label refers to the step. In what follows it will be useful to write the equations in terms of $\tilde{A}_n^{(T)} = A_n^{(T)} - 1$ and $\tilde{B}_n^{(T)} = B_n^{(T)} - 1$. The areas at step $T = 2$ are related each other by:

$$\begin{aligned} &\tilde{A}_1^{(2)} = 3 \cdot \tilde{B}_1^{(2)} + 3 \, , \\ &\tilde{B}_1^{(2)} = \tilde{A}_0^{(2)} + 2 \cdot \tilde{B}_0^{(2)} + 3 \, , \\ &\tilde{B}_0^{(2)} = 0 \, . \end{aligned} \tag{2.83}$$

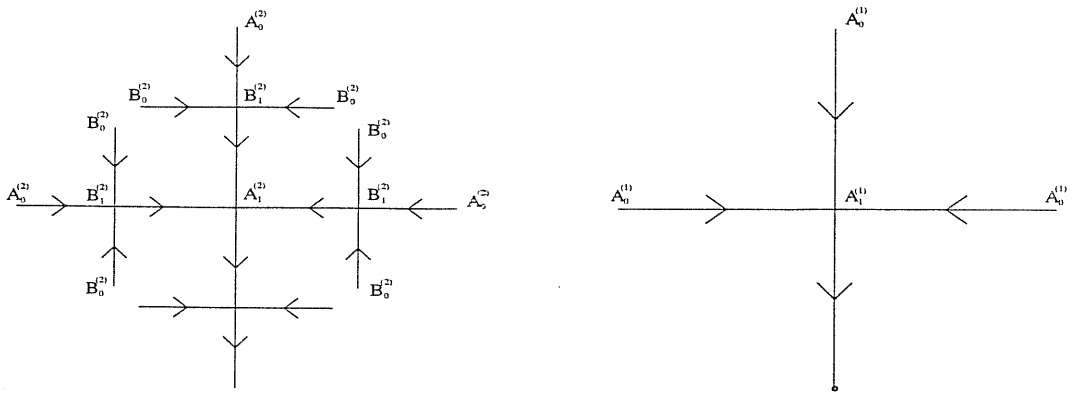

Figure 2.5: Figure 3: The renormalization group argument for the Peano basin. B-sites die under decimation.

Elimination of the $\tilde{B}_n^{(2)}$ leads to

$$\tilde{A}_1^{(2)} = 3 \cdot \tilde{A}_0^{(2)} + 12\,. \tag{2.84}$$

At time step $T = 1$ the relation between areas is straightforward:

$$\tilde{A}_1^{(1)} = 3 \cdot \tilde{A}_0^{(1)} + 3\,. \tag{2.85}$$

Equations (2.84) and (2.85) are the same if

$$\tilde{A}_n^{(T+1)} = 4\,\tilde{A}_n^{(T)}\,, \tag{2.86}$$

i.e.

$$(A_n^{(T+1)} - 1) = 4\,(A_n^{(T)} - 1)\,. \tag{2.87}$$

Denoting with $n^{(T+1)}(a)$ the number of sites with area greater then a at step $T+1$, one can easily observe that the number of decimated sites with $A > a$ is half of the total number of sites with $A > a$

$$n^{(T+1)}(a) = 2 \cdot n^{(T)}(a/4)\,, \tag{2.88}$$

thus, being the total number of sites at step T, $N_T = 4^T$, it follows for the integrated probability $P(A_n^{(T+1)} > a) = \frac{n^{(T)}(a)}{N_T}$:

$$P(A_n^{(T+1)} > a) = b\,P(A_n^{(T)} > \Lambda a) \tag{2.89}$$

with

$$\Lambda = \frac{1}{4} \quad \text{and} \quad b = \frac{n^{(T+1)}(a)/4^{T+1}}{n^{(T)}(a)/4^T} = \frac{2/4^{T+1}}{1/4^T} = \frac{1}{2}\,. \tag{2.90}$$

Equation (2.89) rewritten in terms of $P(a) = \tilde{P}(\log a)$ as

$$\tilde{P}(x) = b\tilde{P}(x + \lambda) \tag{2.91}$$

where $\lambda = \log \Lambda$. The general solution is $\tilde{P}(x) = \exp[(1-\tau)x]w(x)$, where $w(x)$ is a periodic function of period $|\lambda|$ and $\exp[(1-\tau)\lambda] = \Lambda^{1-\tau} = b^{-1}$. Using eq. (2.90) $\tau = \frac{3}{2}$. Then the solution of eq. (2.89) is

$$P(a) = a^{1-\tau} w(\log a) \tag{2.92}$$

Thus an oscillatory term in $\log a$ superimposed to the power law $a^{(1-\tau)}$ might exist and in effect it does.

The same argument can be repeated for the distribution of main stream lengths, recovering the ψ exponent derived in eq. (2.81).

The possible existence of oscillatory terms was first noted by Nauenberg [35] and has been discussed by Niemeijer and van Leeuwen in [36]. They report an argument due to Nelson claiming that oscillatory terms are unlikely to appear because of the fact that two renormalization transformations with opportunely chosen scales factors would lead to incommensurate periods λ_1, λ_2 and thus to a constant $w(x)$. In our case this argument does not apply since we can have only $b = 2^k$, i.e. $\lambda = -\frac{1}{\tau-1} k \log 2$.

In figure (2.6) the log-log plot of $P(a)$ versus a as obtained using eq. (2.75) for the probability density, is shown for a system of linear size $L = 2^{14}$. The dashed line is the power law $a^{(1-\tau)}$ times the scaling function $F(a/L^2)$ of eq.(2.78). In order to highlight the periodicity of the function $w(x)$ of eq.(2.92) in figure (2.7) we draw a log-log plot of $P(a)a^{(\tau-1)} = w(\log a)F(a/L^2)$ versus a. The dashed line is $F(a/L^2)$. The periodicity is $|\lambda| = \log 4$.

The same plots have been done for the mainstream length distribution and are shown in figure (2.8) and (2.9).

Note that the same renormalization group argument can be done in generic dimension d giving $\tau = 1 + \ln d/\ln(2d)$ and $\psi = 1 + \ln d/[2\ln(2d)]$.

We analyzed in detail the Peano basin. The scaling behavior has been worked out exactly. Similar lattice models for rivers has been recently object of extensive studies [37] in which various universality classes have been identified. In particular the mean field theory has been solved through a mapping on the Takayasu random aggregation model [22]. Note that scaling exponents for Peano basin in d=2 result to be the same of this mean field.

A remark needs to be done regarding the generalization in dimension d. One should expect that in the limiting $d \to \infty$ the exponents tend to the mean field ones. Actually this is not the case, in fact one gets $\tau_{d-\infty} = 2$, $\psi_{d-\infty} = 3/2$. This is not surprising, and is due to the

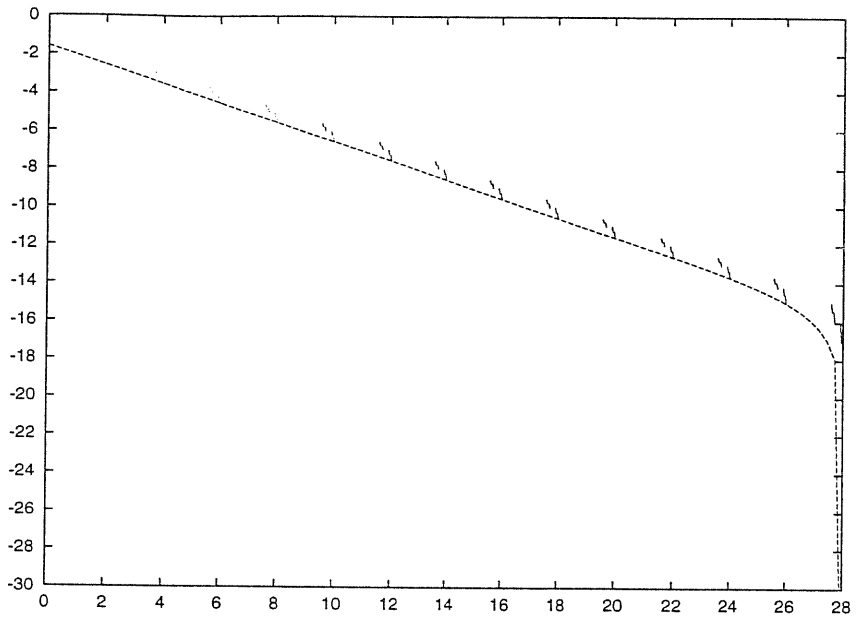

Figure 2.6: Log-log plot of the cumulated areas distribution $P(a)$ versus a for a system of linear size $L = 2^{14}$. The dashed line is $a^{(1-\tau)}F(a/L^2)$.

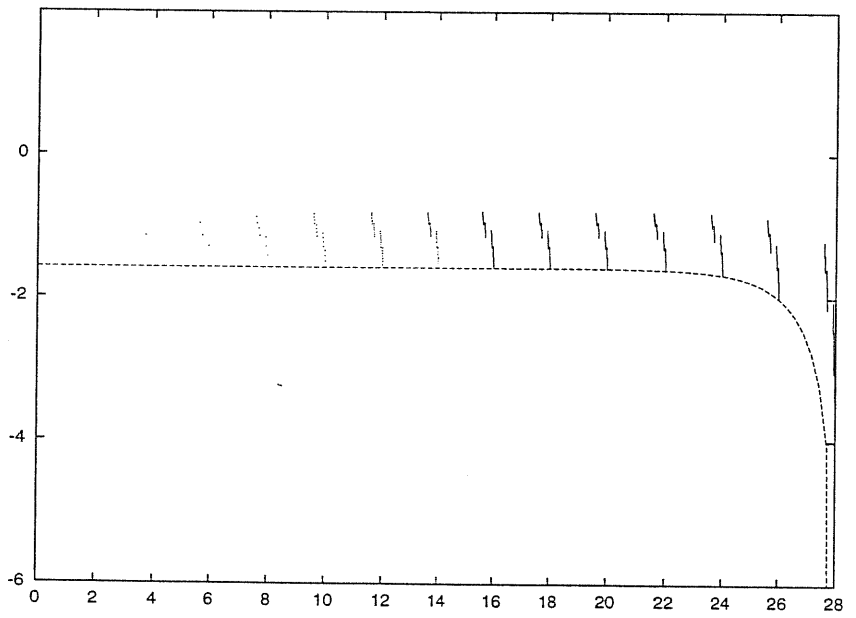

Figure 2.7: Log-log plot of $P(a)a^{(\tau-1)}$ versus a. The dashed line is $F(a/L^2)$ in equation (2.78). The periodicity is $\log 4$.

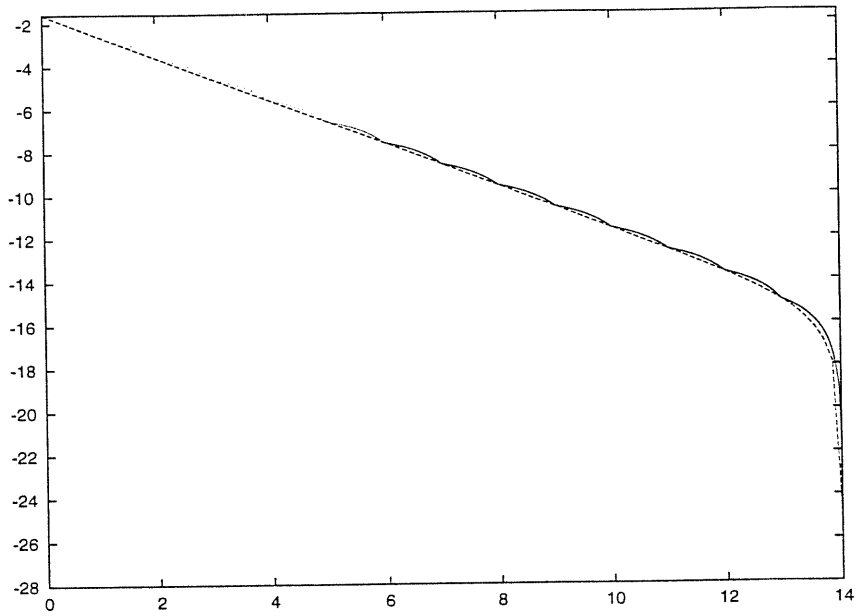

Figure 2.8: The same as in figure 2.6 for the mainstream lengths distribution.

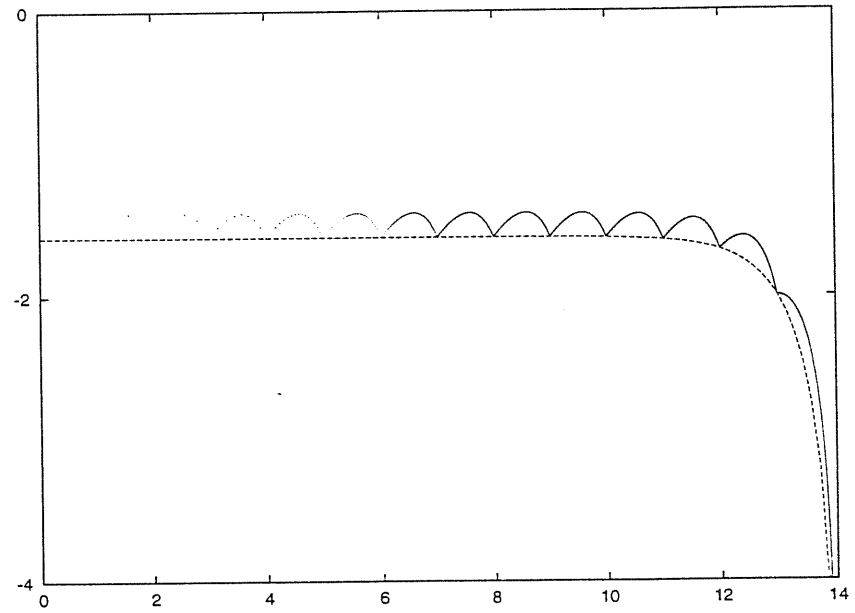

Figure 2.9: The same as in figure (2.7) for the mainstream lengths distribution. Note that in this case the period is $|\lambda| = 1/2$.

fact that in the Takayasu model the tree is space filling only up to dimension $d = 2$ [22] while in Peano basin we impose that by construction in all d.

2.5 Random Spanning Trees

Let's now turn our attention to the set of all spanning trees over a lattice, i.e. the set of all graphs such that any two points result to be connected and no loops are allowed.

This kind of structure emerge in a wide class of problem in Statistical Mechanics: it was shown, for example, by Kirchoff [38] that the spanning tree problem is related to the problem of determining the effective resistance between two nodes of a Resistor Network. It has also been shown by Fortuyn and Kasteleyn [39] that this problem is related to the Potts model in the limit of zero states.

Dhar and Majumdar [40] showed that a one to one correspondence exists between the set of spanning trees over a square lattice and the set of recurrent states in an Abelian sand-pile over the same lattice.

In the context of river networks, a spanning tree is the most general structure which can arise from a field of elevations like DEM. Indeed, if a graph is constructed from an elevation field without lakes considering in each point the oriented link in the direction of steepest descent there will be only a path from each site to the outlet and no loops will be present.

We are now mainly interested in the geometric properties of such structures. We will see how the exponents characterizing the power-law tails of the distributions of cumulated area and of upstream length can be computed and that relations (2.19) and (2.25) also in this case holds.

The fractal dimension has been found by Coniglio [25] to be $d_l = \frac{5}{4}$. The exponent τ and ψ can be deduced by the following renormalization argument due to Manna, Dhar and Majumdar [41].

Let's consider the decimation procedure that at time step $t + 1$ deletes from the tree all that sites that after time step t have just one link touching them. With these procedure, given a tree, we can associate to each site a 'burning time' that is the step of the decimation procedure at which the site is deleted from the tree. For any spanning tree configuration $\mathcal{T}$ a decimated tree $\mathcal{T}'$ can be constructed where the 'burning times' are rescaled by an integer factor b by deleting all sites whose 'burning times' are not exact multiples of b. The remaining sites are connected each other to form a spanning tree over the undecimated sites, and site i will result to be upstream with respect to j on $\mathcal{T}'$ if and only if it is upstream with respect to j on $\mathcal{T}$. Observing that the distribution of 'burning times' has a power law tail, the tree $\mathcal{T}$ and $\mathcal{T}'$ are expected to be similar statistically for large b except for an over

all scale factor.

Note that, in 'river language' the upstream length for a site and its 'burning time' are synonymous.

Let a be the linear rescaling factor corresponding to a rescaling of 'burning times' by b. There are then b links between two adjacent undecimated nodes.

As the fractal dimension of the chemical path between two nodes, i.e of the only path (regardless of orientation of links) which join two nodes on a spanning tree is $\frac{5}{4}$, the average Euclidean distance between two undecimated nodes scales as $b^{\frac{4}{5}}$, or in other words, $a \sim b^{\frac{4}{5}}$. Let's consider the set of sites whose burning time is greater or equal to b. It consists of the undecimated sites and of the sites on the links between the undecimated sites.

Hence the the fraction of such sites is $a^{-2}b \sim b^{-\frac{3}{5}}$, or equivalently

$$\text{Prob}(l > l_0) \sim l_0^{-\frac{3}{5}} \tag{2.93}$$

which means $\psi = 1 + \frac{3}{5} = \frac{8}{5}$.

The probability that a site chosen at random has drained area s consider that it is equivalent to consider the probability to disconnect a cluster of size s removing a link at random from the tree. Since such cluster is compact ($\Phi = 2$), it will have linear size $\sim s^{\frac{1}{2}}$ and perimeter which scales as $(s^{\frac{1}{2}})^{\frac{5}{4}} = s^{\frac{5}{8}}$.

To consider the probability to have a disconnected cluster of a given perimeter is useful to introduce the dual tree $\mathcal{T}^*$ of the primitive tree T we are studying.

Suppose that the tree T is over an infinite square lattice whose sites have integer coordinates. The dual lattice will be the set of all points with half integer coordinates. $\mathcal{T}^*$ is the spanning tree constructed by drawing all links connecting sites of the dual lattice which do not intersect any link of primitive tree T. It exists a $1-1$ correspondence between the set of primitive trees and the set of their duals. The probability to have a disconnected cluster of a given perimeter p by removing a link at random from the primitive tree T is the same of having a loop of length p by adding in the dual tree $\mathcal{T}^*$ the link corresponding (i.e. intersected) by the one removed in T,see figure (2.10). The probability of generating a loop of length p by adding a link in $\mathcal{T}^*$ scales as the 'burning time' (or the main stream length) of the site in which the link is added. Since the distribution of 'burning times' is the same on the primitive tree and on its dual, one find

$$\text{Prob}(A \geq s) \sim Prob(l \geq s^{\frac{5}{8}}) \sim (s^{\frac{5}{8}})^{-\frac{3}{5}} \sim s^{-\frac{3}{8}}. \tag{2.94}$$

which means $\tau = 1 + \frac{3}{8} = \frac{11}{8}$.

Summarizing the distributions of drained area and of upstream length are characterized by:

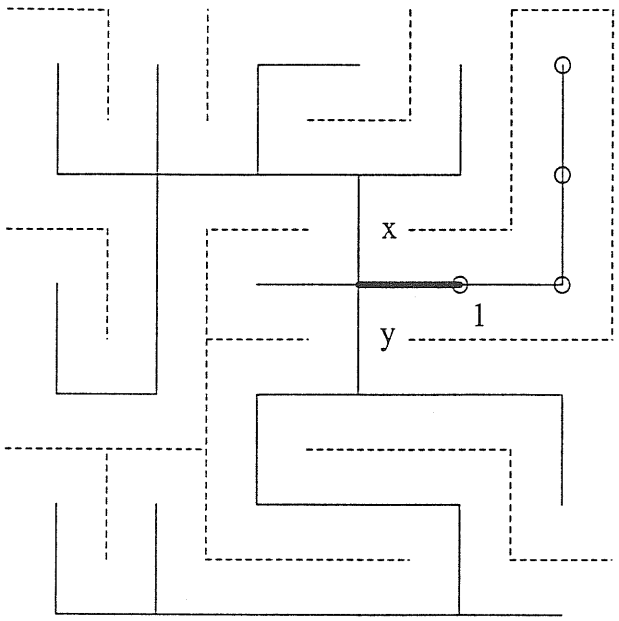

Figure 2.10: A small portion of an infinite random spanning tree (continues line) and of its dual (dashed line). The drained area in site 1 is the number of sites which become disconnected if the bold link is removed. The perimeter of the disconnected cluster coincide with the the loop generated by adding link (x, y) in the reciprocal tree, i.e. the reciprocal of the bold link in the direct tree.

$$\tau = 11/8\,, \psi = 8/5\,, \Phi = 2\,, d_l = 5/4\,, h = 5/8\,, \tag{2.95}$$

Note that the exponents above can be simply found by using our scaling relations and by the knowledge of the fractal dimension d_l. Moreover scaling relation (2.19) and (2.25) holds for different class of spanning trees, while the argument exposed here is peculiar for the case of all spanning trees because it is based on the self-duality of this set.

3 Optimal Channel Network

DEM provided a powerful tool to describe and characterize the geometrical features of river basins. Thanks to them has been possible to measure the distribution of drained area and of upstream length for a large number of basins in the most different conditions from the point of view of climate, ubication, soil characteristics and size of the basin.

One of the most striking feature shown by the huge amount of data coming from DEM is that, despite of the great difference of geological conditions, river basins are very close one to each other from the point of view of geometrical structure. The power-law tails of the distributions of cumulated area and of main stream length, which are the signature of their fractal behavior, have to a large extent the same value in all the cases considered.

The observation of this kind of 'universal behavior' made geologists confident that a simple model can be formulated to explain also quantitatively the geometrical features of river basins, without taking into account all that environmental details which are so different from a basin to another.

The model for river network we analyze in the remaining part of this work is called Optimal Channel Network (OCN) and has been introduced some years ago by Rinaldo and Iturbe [14, 15]. It is based on the principle that river basin evolve to realize a network in which the energy dissipated is minimized.

The idea that drainage structure in Nature can arise from optimality principles is not new, see for example [42]. Lot of example are therein contained, showing how several systems in which drainage is involved (the blood flow in vessels, the air in leafs) develop branched structures whose characteristics can be recovered assuming a principle of minimal energy expenditure.

The discussion of this principle goes beyond the aim of this work, and we will limit ourself, before formulating OCN model, to discuss the example of Resistor Networks. These dissipative systems show a close resemblance with the problem of water drainage in river basin and their behavior can be completely recovered by mean of a principle of minimal energy expenditure.

In Section 3 we will derive exactly the scaling behavior of OCN model in the homogeneous case, i.e. under the assumption that precipitation and soil properties are the same all over the basin.

Different universality classes will arise depending on the parameter γ in the expression of the dissipated energy. In the physical case $\gamma = 1/2$ we find the same exponents as in the mean field case of Scheiddeger model and in the Peano basin case.

In Section 4 the presence of disorder is considered. We will see to which extent it is irrelevant from the point of view of scaling behavior and when, instead, it leads to a new set of scaling exponents.

3.1 Resistor Networks

A Resistor Network is a generic graph whose links are resistors and whose vertices are nodes, i.e. points in which two or more resistors join. We will indicate with R_{ij} the resistance of resistor joining node i and node j, with V_i the electric potential at node i, and with q_{ij} the intensity of current flowing from node i to node j when a difference of of electric potential is established at two nodes of the resistor.

Using Kirchoff's and Ohm's law the current in each link and the potential in each node can be calculated, once the potential is given at the two ends. These two laws state:

Kirchoff law: The sum of all currents incoming in a node is equal to 0, apart from the nodes in which the current is injected from outside or it is ejected from the system.

$$\sum_j q_{ij} = q_0 \delta_{i,i_0} - q_1 \delta_{i,i_1} \quad \forall i \tag{3.1}$$

where q_0 is the current ejected from the system at the node i_0 and q_1 is the current injected from outside in the site i_1, further $q_{i,j} = -q_{j,i}$.

Ohm law: The current flowing in a link is proportional through its resistance to the difference of potential between the two ends of the link.

$$V_{ij} = R_{ij} q_{ij} \quad \forall i,j \tag{3.2}$$

Kirchoff law is a continuity equation for the electric charge, while Ohm's law can be easily recovered assuming that currents are such to minimize the energy dissipation in the whole network and the constraint that in each site the incoming and the out-coming current in a node must be the same.

The energy dissipated by a resistor of resistance R is given by $E = Rq^2$ where q is the current flowing in the resistor. The whole net will then dissipate:

$$E = \frac{1}{2}\sum_{i \neq j} R_{ij} q_{ij}^2. \tag{3.3}$$

Then the equations for the currents which minimize the dissipated energy and at the same time satisfy constraint given by Kirchoff's law will reads:

$$\frac{d}{dq_{ij}}(\frac{1}{2}\sum_{i \neq j} R_{ij} q_{ij}^2) + \sum_i \lambda_i (\sum_j q_{ij}) = 2R_{ij} q_{ij} + \lambda_i - \lambda_j = 0. \tag{3.4}$$

From relation above Ohm's law follow identifying the Lagrangian multiplayer λ_i with electric potential in site i. The stationary point given by equation (3.4) can be shown to be a minimum for functional (3.3), see for example [43].

3.2 Optimal Channel Network

The Optimal Channel Network model is based on two assumptions founded on experimental evidence and on the principal of minimal energy dissipation. It can be formulated as follow:

i) Constant velocity:

the velocity of water is constant in each point of the basin.

ii) area-discharge law:

If we call $h(\underline{x})$ the height of the landscape at point $\underline{x}$, the water flux $\vec{Q}(\underline{x})$ is in the direction of the steepest descent, i.e.

$$\vec{Q}(\underline{x}) // (\vec{\nabla} h(\underline{x}), -\frac{1}{1 + |\vec{\nabla} h(\underline{x})|^2}).$$

In each point the modulus of the gradient is proportional to a power of the quantity of water Q(x) flowing in the point.

$$|\vec{\nabla} h(\underline{x})| = k(\underline{x}) |\vec{Q}(\underline{x})|^{\gamma - 1} \doteq Q(\underline{x})^{\gamma - 1}$$

where $k(\underline{x})$ is the proportionality constant which depends on $\underline{x}$ and $1 - \gamma$ has an experimental value of about 0.5.

iii Principle of minimal energy expenditure:

the network in its stationary state assume a configuration in which a minimum of dissipated energy is reached.

Assumption *i*) implies that all the potential energy of water injected in the system by precipitation is dissipated by friction, infact constant velocity along the flow means no gain or loss in kinetic energy. Given the elevation field $h(\underline{x})$, the flow $\vec{Q}(\underline{x})$ can be computed by assumption *ii*) stating it is directed along the direction of steepest descent and from the equation of continuity:

$$\mathrm{div}\vec{Q}(\underline{x}) = r(\underline{x}), \tag{3.5}$$

where $r(\underline{x})$ is the precipitation in $\underline{x}$. The dissipated energy can be calculated as the potential energy loose by water flowing downstream, and by mean of assumption *ii*) it reads:

$$E(\vec{Q}(\underline{x})) = \int Q(\underline{x})|\vec{\nabla}h(\underline{x})|d\underline{x} = \int Q(\underline{x})^{\gamma}k(\underline{x})d\underline{x}. \tag{3.6}$$

In what follow we will deal with the discrete version of this model. Let $\mathcal{L}$ be a lattice. If h_i is the eight of landscape at site i, the set of draining directions $\{\vec{Q}_i\}$ will be given as usual, by the oriented links which join each point with its nearest neighbor with smallest height.

Once the set of draining directions is given, the quantity of water flowing in a point can be computed as

$$Q_i(\mathcal{T}) = \sum_{j \in up(i)} r_j, \tag{3.7}$$

where the sum over j runs over all sites which are upstream respect to site i. The dissipated energy can also be computed from drainage directions as

$$E(\mathcal{T}) = \sum_{i \in \mathcal{L}} Q_i(\mathcal{T})|h_i - h_j| \tag{3.8}$$

where j is the site toward water is flowing from i and T is the spanning tree determined by the set of drainage directions $\{\vec{Q}_i\}$. Assuming as in *ii*) that $|h_i - h_j| = k_i Q_i^{\gamma-1}$ we find:

$$E(\mathcal{T}) = \sum_{i \in \mathcal{L}} k_i Q_i(\mathcal{T})^{\gamma}. \tag{3.9}$$

In this discretized version, calling S the set of all spanning tree over the lattice L the principal of minimal energy expenditure can be formulated as follow:

Principle of minimal energy dissipation: The network in its stable configuration is given by the spanning tree T which realize a minimum for the functional

$$E(T) = \sum_{i \in \mathcal{L}} k_i Q_i(T)^{\gamma}. \tag{3.10}$$

.

Aim of the following Sections is to work out the scaling properties of the spanning trees which realize the absolute minimum for the functional (3.10). Two set of parameters are involved in this problem; namely the r_i which represent the water injected at point i and the k_i which take into account the inhomogeneities in the soil properties. To begin we will consider both r_i and k_i as constants and then we will discuss what changes for the distributions of drained area and of upstream length considering R_i and k_i uncorrelated random variables. Moreover functional (3.10) depends on the parameter γ relating the slope and the quantity of water flowing in a point. Experimental observations give for γ a value which is around 0.5. We will study the problem for $\gamma \in [0, 1]$ to understand how robust are the scaling properties of the "minimal tree" for different γ.

Before proceeding let's stress the analogies between the problem of OCN and of Resistor Networks.

If we neglect for a while the assumption that from each site water can flow in just one direction, i.e. the direction of steepest descent, a close analogy can be established between this generalized version of OCN and Resistor Networks: we can identify the current q_{ij} flowing in the link $i-j$ with Q_{ij} (we call Q_{ij} the water flowing in the link $i-j$ if more than one drainage direction is allowed), the electric potential V_i with the eight of the landscape h_i and the erodability k_{ij} with the resistance R_{ij}.

In both cases we have a network and, for each site, an equation of continuity holds. In both cases we are asked to find the set of currents which minimize the dissipated energy. The fundamental difference in these two problems stands in the parameter γ appearing??? in the form of the functional to be minimized.

In the case of Resistor Network $\gamma = 2$ in functional (3.10) together with the continuity equations gives place to Ohm's law which allows to completely solve the resistor; in other words only a minimum is found for equations (3.1) and (3.4).

Also in the case of generalized [44, 45] OCN one can derive from continuity equation and from the principle of minimal energy expenditure the area-discharge relation which relates the flow and the differences in height and that is the analogous of Ohm's law for OCN.

In the case of OCN the fact that power γ in functional (3.10) is between 0 and 1 gives place to a very complicated "energy landscape" extremely rich of local minima.

Recently Maritan et al [45] showed that in this generalized version of OCN (multiple flow directions allowed in a point) local minima for the dissipated energy arise when water flows out from a point just through a link, so that it's not a restriction to consider only the case

of flow in the direction of steepest descent, i.e only network spanning-tree like.

We conclude noting that in the case of OCN the principle of minimal energy expenditure contains a stronger claim if compared with the analogous for Resistor Network: while in the latter case only one minimum is found for the dissipated energy and it give the physical solution of the problem, lot of local minima arise minimizing the dissipated energy for OCN. These local minima are realized by configuration in which all the water incoming in a site is drained through only one link and that's why we can consider only spanning tree configurations without loose in generality.

The claim of the optimality principle is, then, that only the local minima with the lowest energy are realized in Nature.

3.3 Scaling properties of OCN: homogeneous case

We now proceed to an analysis of the characteristic of the global minimum of the functional E for γ in the range $[0,1]$ for the homogeneous case, i.e we will assume, if not different stated that $r_i = 1$ and $k_i = 1$. Note that with these assumption the quantity of water Q_i flowing in a point is proportional to the drained area A_i in that point and that the energy dissipated by a tree $\mathcal{T}$ is given by:

$$E(\mathcal{T}) = \sum_i A_i^{\gamma}. \tag{3.11}$$

Let us consider first the two limiting cases $\gamma = 0$ and $\gamma = 1$. If we call l_i the weighted length of the stream connecting the i-th site to the outlet (calculated assigning to each bond a length k_i), it is straightforward to show that

$$\sum_i k_i A_i = \sum_i l_i \,. \tag{3.12}$$

In effect, denoting with $DS(i)$ ($US(i)$) the set of points downstream (upstream) with respect to the point i and observing that $A(i)$ equals the number of points in the set $US(i)$ one gets: $\sum_i l_i = \sum_i \sum_{j \in DS(i)} k_j = \sum_j \sum_{j \in US(i)} k_j = \sum_i k_i A_i$.

The minimization of the energy dissipation for $\gamma = 1$ thus corresponds to the minimization of the weighted path connecting every site to the outlet independent of each other.

The $\gamma = 0$ case, on the other hand, corresponds to the minimization of the total weighted length of the tree:

$$E = \sum_i k_i \,. \tag{3.13}$$

In the homogeneous case $k_i = 1, \forall i$, which leads to a high degeneracy for both $\gamma = 0$ and 1.

Indeed for $\gamma = 0$, each configuration has the same energy (each spanning tree on a $L \times L$ square lattice has $L^2 - 1$ links). For $\gamma = 1$, the minimum of the energy is realized on a large subclass of spanning trees, namely all the *directed* trees, in which each link has a positive projection along the diagonal oriented towards the outlet.

For the values of $\gamma \in (0,1)$ there is a competition between both mechanisms breaking the degeneracy and making the search for the global minimum a less trivial problem.

The $\gamma = 1$ case gives a minimum energy $E \sim L^3$. This can be derived observing that all points on a diagonal orthogonal to the one passing through the outlet have the same distance from the outlet. Then: $E = \sum_{k=1}^{L-1} k(k+1) + \sum_{k=L}^{2L-2} k(2L-1-k) = L^2(L-1) \sim L^3$. Thus the value of the energy functional is the same for each *directed* network and corresponds to the Scheiddeger model of river networks [20] - all *directed* trees are equally probable. Such a model can be mapped into a model of mass aggregation with injection that has been exactly solved by Takayasu et al. [22, 21]. The corresponding exponents are:

$$\tau = 4/3\,, \psi = 3/2\,, H = 1/2\,, d_l = 1\,, h = 2/3\,. \tag{3.14}$$

These exponents follow easily from the result $H = 1/2$ and from our scaling solution of sec. 2. The result $H = 1/2$ can be deduced with a simple argument: since all *directed* trees are equally probable, each stream behaves like a single random walk in the direction perpendicular to the diagonal through the outlet. This implies that its perpendicular wandering is $L_\perp \sim L^{1/2}$. Comparing with equation (2.5) one gets $H = 1/2$.

The $\gamma = 0$ case leads to the same energy $E \sim L^2$ for each network, thus reducing to the problem of random two dimensional spanning trees, whose geometrical properties have been calculated on a square lattice [26, 25]. The results, in our notation, are:

$$\tau = 11/8\,, \psi = 8/5\,, H = 1\,, d_l = 5/4\,, h = 5/8\,. \tag{3.15}$$

Both (3.14) and (3.15) are consistent with the scaling relations (2.26)), (2.27) and (2.28).

We now extend our analysis to the whole range $\gamma \in [0,1]$. We will rigorously show that, in the thermodynamic limit, the global minimum in the space $\mathcal{S}$ of all the spanning trees of the functional $E(\gamma, \mathcal{T}) = \sum_i A_i(\mathcal{T})^\gamma$ scales as

$$\min_{\mathcal{T} \in \mathcal{S}} E(\gamma, \mathcal{T}) \sim \max(L^2, L^{1+2\gamma}) \tag{3.16}$$

for all $\gamma \in [0,1]$.

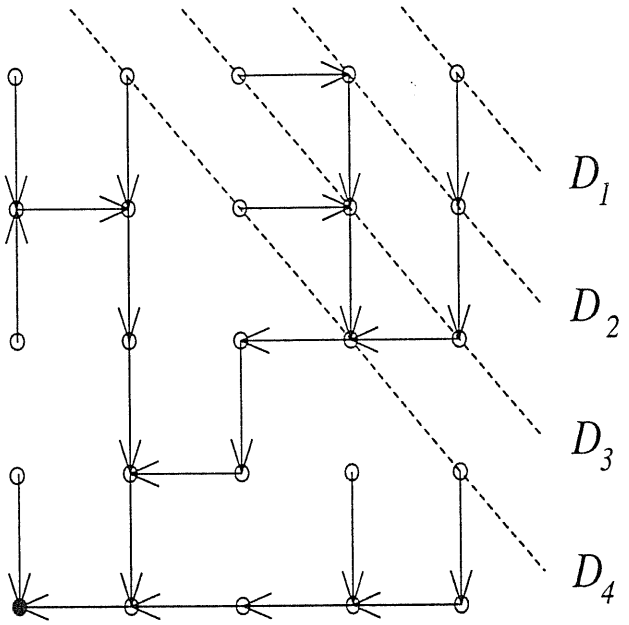

Figure 3.1: Each dashed line divides the lattice in two parts. $\sum_{i\in\mathcal{D}} A_i$ is at least equal at the number of sites contained in the part of the lattice with border $\mathcal{D}$ and without the outlet.

Since $E(\gamma,\mathcal{T})$ is an increasing function of γ and it is equal to L^2 for $\gamma = 0$, for $\gamma \geq 0$ it is obvious that

$$E(\gamma,\mathcal{T}) \geq L^2 \,. \tag{3.17}$$

We now observe that the sum over all the sites can be performed in two steps:

$$E(\gamma,\mathcal{T}) = \sum_{n=1}^{2L-1} \sum_{i\in\mathcal{D}_n} A_i(\mathcal{T})^\gamma \tag{3.18}$$

where $\mathcal{D}_n$ are the lines orthogonal to the diagonal passing through the outlet, that we will enumerate starting from the corner farthest from the outlet, see figure (3.1). For *directed* spanning trees one can observe that the sum of the areas in a given line $\mathcal{D}_n$ is independent of the particular tree, and is:

$$S_d(k) \doteq \sum_{i\in\mathcal{D}_k} A_i = \begin{cases} k(k+1)/2 & k \leq L \\ L^2 - S_d(2L-1-k) & L+1 \leq k \leq 2L-1 \end{cases} \tag{3.19}$$

Let us observe that for $k = 0, ..., (L-1)$:

$$S(k,\mathcal{T}) + S(2L-1-k,\mathcal{T}) \geq S_d(k) + S_d(2L-1-k) = L^2 \,, \tag{3.20}$$

making it convenient to perform the summation in (3.18) over "pairs" of lines. To get a lower bound for E we need a further inequality: for every set Γ

$$\sum_{i\in\Gamma} A_i^\gamma \geq (\sum_{i\in\Gamma} A_i)^\gamma \,, \tag{3.21}$$

that follows easily from Schwartz inequality, since $A_i \geq 1$ and $0 \leq \gamma \leq 1$. Now, using (3.18), (3.20) and (3.21) we can write:

$$\begin{aligned} E(\gamma,\mathcal{T}) &= \sum_{n=1}^{2L-1}\sum_{i\in\mathcal{D}_n} A_i(\mathcal{T})^\gamma = \sum_{n=0}^{L-1}\sum_{i\,\in(\mathcal{D}_n\cup\tilde{\mathcal{D}}_n)} A_i^\gamma \geq \sum_{n=0}^{L-1}(\sum_{i\,\in(\mathcal{D}_n\cup\tilde{\mathcal{D}}_n)} A_i(\mathcal{T}))^\gamma \\ &= \sum_{n=0}^{L-1}[S(n,\mathcal{T})+S(2L-1-n,\mathcal{T})]^\gamma \geq \sum_{n=0}^{L-1} L^{2\gamma} = L^{1+2\gamma}\,, \end{aligned} \tag{3.22}$$

where $\tilde{\mathcal{D}}_n = \mathcal{D}_{(2L-1-n)}$. The equality in the last inequality holds for *directed* networks. We can thus write

$$E(\gamma,\mathcal{T}) \geq L^{1+2\gamma}\,. \tag{3.23}$$

Equation (3.23) together with the (3.17) gives the lower bound

$$E(\gamma,\mathcal{T}) \geq \max(L^2, L^{1+2\gamma})\,, \tag{3.24}$$

that holds for every $\mathcal{T}\in\mathcal{S}$ and thus also for the minimum over $\mathcal{T}$. Using the results of the previous Section, we can exhibit a tree on which the bound is realized. In effect, the Peano network can be mapped on a square lattice only considering links between first and second nearest neighbors, but (3.24) can be analogously obtained for such a lattice on rearranging in an opportune way the summation in equation (3.18). If we call $\mathcal{T}_P$ the spanning tree given by the Peano basin we know that, except for logarithmic corrections for $\gamma = 1/2$, $E(\gamma,\mathcal{T}_P) \sim \max(L^2, L^{1+2\gamma})$. Infact the mean value of A_i^γ for a Peano basin of size $L = 2^t$ can be calculated as follow

$$\langle A^\gamma\rangle = \frac{1}{L^2}\sum_i A_i^\gamma = \sum_{n=0}^{\infty} p_T(a_n) {a_n}^\gamma\,. \tag{3.25}$$

From the expression for a_n, it follows that

$$\frac{3}{4}\cdot 4^{t(a_n)} < a_n \leq 4^{t(a_n)} \tag{3.26}$$

($t(a_n)$ is the "birth-time" for a_n), giving

$$\left(\frac{3}{4}\right)^{\gamma} \alpha(L=2^T) \leq \langle A^{\gamma} \rangle \leq \alpha(L=2^T), \tag{3.27}$$

where

$$\alpha(L=2^T) \doteq \frac{2}{3} + \frac{1}{34^T} + \sum_{t=1}^{T} \left(\frac{2}{3} 4^{(T-t)} + \frac{1}{3}\right) \frac{2^{t-1}}{4^T} 4^{\gamma t}. \tag{3.28}$$

Performing the summation one gets in the large size limit

$$\alpha \sim \begin{cases} \frac{1}{3}(1 + \frac{1}{1-2^{2\gamma-1}}) & , \quad \gamma < 1/2 \\ \frac{1}{3\log 2} \log L & , \quad \gamma = 1/2 \\ \frac{1}{1-2^{1-2\gamma}} L^{2\gamma-1} & , \quad \gamma > 1/2 \end{cases} \tag{3.29}$$

From equation (3.27), one gets

$$\langle A(L)^{\gamma} \rangle \sim \begin{cases} const & \gamma < 1/2 \\ \log L & \gamma = 1/2 \\ L^{2\gamma-1} & \gamma > 1/2 \end{cases} \tag{3.30}$$

which will be essential to obtain an energy bound for the lattice OCN model.

$$\min_{T \in \mathcal{S}} E(\gamma, T) \leq E(\gamma, \mathcal{T}_P), \tag{3.31}$$

and we get equation (3.16).

We now proceed to the calculation of the scaling exponents.

For a directed path, from equation (3.12),

$$\langle a \rangle \sim L. \tag{3.32}$$

For generical "undirected" networks, let us write as in (2.18)

$$\langle a \rangle \sim L^{d_l} \tag{3.33}$$

Using eq. (2.10) with $n = \gamma$ and the above result on the scaling of energy: $E = L^2 \langle a^{\gamma} \rangle \sim L^{1+2\gamma}$, one gets

$$2\gamma - 1 = (1 + H)(\gamma - \tau + 1) \tag{3.34}$$

holding for $\gamma > \tau - 1$.

Equations (3.34) together with the scaling relation (2.19) can be solved with respect to τ and H, and gives, for $\gamma > 1/2$

$$\begin{cases} \tau = \frac{3(1-\gamma)+(d_l-1)(1+\gamma)}{2(1-\gamma)+d_l-1} \\ H = \frac{d_l-\gamma}{1-\gamma} \end{cases} \tag{3.35}$$

(the constraint $\gamma > \tau - 1$ become $\gamma > 1/2$, independently of d_l). Thus, if $H \leq 1$, for any $\gamma < 1$ $d_l = 1$, yielding

$$\tau = 3/2 \ , \ H = 1 \ , \ \psi = 2 \ , \ d_l = 1 \ , \ h = 1/2 \tag{3.36}$$

for $\gamma \in (1/2, 1)$. The exponents are the same as in the mean field theory [22, 21] of the Scheidegger model and the same as in the Peano case.

Note that equations (3.35) are meaningless for $\gamma = 1$, in which case (3.36) does not hold, consistent with the Scheiddeger results (3.14).

When $0 < \gamma < 1/2$, all we can say is that $\tau > 1+\gamma$. However if $d_l = 1$ for any $\gamma \in (0, 1)$ (i.e. the Optimal Channel is *quasi − directed*) then one might expect that $H = 1$ for all values of γ and thus eq. (3.36) holds in the whole range $\gamma \in (0, 1)$. This prediction is confirmed by results of numerical simulations.

3.4 Scaling properties of OCN: heterogeneous case

In this Section we focus our attention on the case in which some sort of quenched disorder is present in the basin. Two cases have been analyzed:

i) random bonds, modeling heterogeneity in the local properties of the soil;

ii) random injection, modeling non-uniformity in the rainfall.

In the first case, we will show that the energy can be bounded from above with the corresponding one in the absence of disorder. This will give in the large L limit an upper bound for the τ exponent that we will see is realized for all the $\gamma \in (1/2, 1)$. In the case of random rainfall, we will show that this kind of randomness does not affect the scaling behavior of the dissipated energy in the large L limit. All the analytical results found in Section 3 for the homogeneous case, being based on the energy estimate in the thermodynamic limit, can thus be extended to that case,giving the same values for the exponents.

In the case of random bonds, we associate with each bond of the $L \times L$ square lattice ($2L(L-1)$ bonds) a quenched random variable k_b, arbitrarily distributed such that $\langle k_b \rangle = 1$. The label b ranges over all the bonds of the lattice. The $2L(L-1)$ variables are chosen independent of each other and identically distributed.

In what follows $b(i,\mathcal{T})$ will denote the label associated with the bond coming out from the site i on the tree $\mathcal{T}$. Let $\mathcal{T}^*(\gamma)$ denote one of the trees on which the minimum of the energy $E(\gamma,\mathcal{T})$ is realized in the homogeneous case for a given value of γ, and S the set of all the spanning trees:

$$E(\gamma) \doteq \min_{\mathcal{T}\in\mathcal{S}} E(\gamma,\mathcal{T}) = \sum_i A_i(\mathcal{T})^\gamma = \sum_i A_i(\mathcal{T}^*(\gamma))^\gamma . \tag{3.37}$$

Denoting by $E_D(\gamma)$ the minimum of the energy in the heterogeneous case, averaged over the quenched disorder, the following inequality holds:

$$\begin{aligned} E_D(\gamma) &\doteq \langle \min_{\mathcal{T}\in\mathcal{S}} \sum_i k_{b(i,\mathcal{T})} A_i(\mathcal{T})^\gamma \rangle \le \langle \sum_i k_{b(i,\mathcal{T}^*(\gamma))} A_i(\mathcal{T}^*(\gamma))^\gamma \rangle \\ &= \langle \sum_i k_{b(i,\mathcal{T}^*(\gamma))} \rangle A_i(\mathcal{T}^*(\gamma))^\gamma = \sum_i A_i(\mathcal{T}^*(\gamma))^\gamma = E(\gamma) . \end{aligned} \tag{3.38}$$

The energy in the presence of this kind of disorder is thus bounded from above by the energy in the absence of disorder for any value of the γ parameter. In the large size limit this result gives bounds on the scaling exponents. Equation (2.10) evaluated for $n = \gamma$ gives

$$\langle a^\gamma \rangle \sim L^{(1+H_D)(\gamma-\tau+1)} \tag{3.39}$$

which holds for any $\gamma > \tau_D - 1 = 1 - h_D$, thus at least for any $\gamma > 1/2$ since $h_D \ge 1/2$. Here and in what follows variables with the D index refer to the random bond case. Equation (3.39), compared with equation (3.16) leads to

$$(1 + H_D)(\gamma - \tau_D + 1) + 2 \le 1 + 2\gamma \quad , 1/2 \le \gamma \le 1. \tag{3.40}$$

In the case of self-affine behavior, using eq. (2.19), equation (3.40) gives:

$$H_D \ge 1 \quad , 1/2 \le \gamma < 1. \tag{3.41}$$

As before, for the $\gamma = 1$ case the above inequalities are useless. In the case of self similar behavior, inequalities for the fractal dimension $d_{l,D}$ can analogously be deduced:

$$d_{l,D} \le 1 \quad , 1/2 \le \gamma \le 1 \tag{3.42}$$

Because, in general $0 \le H \le 1$ and $1 \le d_l \le 1 + H$, equations (3.41) and (3.42) Together yield for $\gamma \in (1/2, 1)$:

$H_D = 1$, $d_{l,D} = 1$, i.e. the mean field values.

In order to calculate the scaling exponents in the case $\gamma = 1$ with disorder in the soil properties, i.e. when to each bond is associated a random variable $k_{i,j}$ we can proceed as follow. First note that the functional to be minimized in this case reads:

$$E = \sum_i k_i A_i \tag{3.43}$$

where k_i is the random variable associated to the link outgoing from i in the tree considered. We already showed that it can be rewritten as:

$$E = \sum_i l_i \tag{3.44}$$

where l_i is the distance along the tree of site i from the outlet, and where

$$l_i = \sum_{j \in ds(i)} k_j \tag{3.45}$$

with index j running over all sites downstream of i.

One can expect that single streams, in the limit of large sizes of the basin have a direct character because tortuos paths are much more unlikely from energetic point of view. Therefore, without loss of generality we can restrict the set in which we search the 'minimal' tree to the direct ones. For such trees the length of each single path can be minimized independently from the others.

The above statement can be understood by iteration. Consider the usual set D_i of diagonals orthogonal to the one going through the outlet as in figure (3.1). Start from the sites lying on D_{2L-2}. They have just one possible choice to reach the outlet. Consider then the sites on diagonal D_{2L-3} and connect each of them to the site (between the two that can be chosen on diagonal D_{2L-2}) with smaller l. Then iterate the above procedure just substituting diagonal D_{2L-2} with diagonal D_{2L-k} and diagonal D_{2L-3} with D_{2L-k-1}. In this way the length of each path to the outlet can be optimized.

To calculate exponent H we note that the sub-basin of a generic site i, i.e. the set of all points upstream of i is bounded by two paths obtained with the iterative method we just described. Therefore the H exponent can be identified with the exponent which describes the wondering of the optimal path around its mean position.

The scaling behavior of these optimal paths is a well known problem in Statistical Mechanics. It is called problem of the Direct Polymer in Random Media (DPRM) and it is connected to the problem of the interface in a bidimensional Ising model with small disorder in the

interactions [46, 47, 48], as well as to the problem of the growth of a surface under random particle deposition.

The wandering exponent for the DPRM has been exactly calculated , see references above and it is $H = \frac{2}{3}$.

Using the scaling relations (2.19) and (2.25) we found for OCN with $\gamma = 1$ with disorder [37]:

$$\tau = 7/5 \ , \ \psi = 5/3 \ , \ H = 2/3 \ , \ d_l = 1 \ , h = 3/5 \ . \tag{3.46}$$

Disorder can be introduced in the system in another way, replacing the constant injection in each site of the lattice with a random, quenched, local injection, i.e. a spatial inhomogeneity in the rainfall r_i in eq. (1.1).

In order to do that, one can associate with each site i of the lattice a random variable r_i. The variables are chosen to be independent of each other, identically distributed and with mean $\langle r_i \rangle = 1$.

The cumulated areas must then satisfy, as in (1.1)

$$A_i = \sum_j w_{i,j} A_j + r_i \ , \tag{3.47}$$

in such a way that

$$A_i = \sum_j \lambda_{i,j} r_j \ , \quad \text{with } \lambda_{i,j} \doteq \begin{cases} 1 & \text{if } i \text{ is connected to } j \\ & \text{through upstream drainage directions} \\ & \text{or if } j = i \ , \\ 0 & \text{otherwise .} \end{cases} \tag{3.48}$$

The minimum of the energy averaged over the "random-rainfall" will be denoted by $E_{rr}(\gamma)$, and for a given value of γ is given by

$$E_{rr}(\gamma) \doteq \langle \min_{\mathcal{T} \in \mathcal{S}} \sum_i A_i(\{r_j\}, \mathcal{T})^\gamma \rangle \ , \tag{3.49}$$

where $\mathcal{S}$ denotes the set of all spanning trees $\mathcal{T}$ and $\{r_j\}$ denotes the whole set of random variables. As in (3.37) $\mathcal{T}^*$ will be one of the trees for which the minimum of the energy is realized in the absence of randomness in the rainfall and for a given value of γ. Then

$$E_{rr}(\gamma) \doteq \langle \min_{\mathcal{T} \in \mathcal{S}} \sum_i A_i(\{r_i\}, \mathcal{T})^\gamma \rangle \leq \langle \sum_i A_i(\{r_i\}, \mathcal{T}^*(\gamma))^\gamma \rangle$$

$$= \langle \sum_i \Big(\sum_j \lambda_{i,j}(T^*(\gamma)) r_j \Big)^\gamma \rangle \leq \sum_i \sum_j \lambda_{i,j}(T^*(\gamma)) \langle r_j \rangle^\gamma$$
$$= \sum_i A_i(T^*)^\gamma = E(\gamma) . \tag{3.50}$$

Thus

$$E_{rr}(\gamma) \leq E(\gamma) \sim \min(L^2, L^{1+2\gamma}) . \tag{3.51}$$

In this case, it is possible to bound the energy also from below with an argument analogous to that used in Section 3 for the homogeneous case.

Using the notation of Section 3 we denote by $\mathcal{D}_n$ the lines orthogonal to the diagonal passing through the outlet, enumerated starting from the corner farthest from the outlet with 0. It will be useful to associate each line $\mathcal{D}_n$ with $n \leq L-1$ with a $\tilde{\mathcal{D}}_n$:

$$\tilde{\mathcal{D}}_n = \mathcal{D}_{(2L-1-n)} . \tag{3.52}$$

In what follows we will choose the $\{r_i\}$ to be independent random variables with values in the interval $[0,2]$ and such that $\langle r_i \rangle = 1$. We then proceed to the first step of the proof as in Section 3, observing that the sum over all the sites in equation (3.49) defining the energy can be performed in two steps:

$$\begin{aligned} E_{rr}(\gamma) &\geq \langle \min_{T \in \mathcal{S}} \sum_i A_i(\{r_i\}, T)^\gamma \rangle \\ &\geq \langle \min_{T \in \mathcal{S}} \sum_{n=0}^{L-1} \Big(\sum_{i \in (\mathcal{D}_n \cup \tilde{\mathcal{D}}_n)} A_i(\{r_i\}, T) \Big)^\gamma \rangle \\ &\geq \sum_{n=0}^{L-1} \langle \Big(\sum_{k=1}^{n} \sum_{i \in \mathcal{D}_k} r_i + \sum_{k=1}^{2L-1-n} \sum_{i \in \mathcal{D}_k} r_i \Big)^\gamma \rangle , \end{aligned} \tag{3.53}$$

where in the last step the equality holds only for directed trees.

The last expression can be written in a more convenient form introducing

$$\mu_i = \begin{cases} 2 & i \in \mathcal{D}_k , \text{ with } k \leq n \\ 1 & \text{otherwise} . \end{cases} \tag{3.54}$$

Then

$$E_{rr} \geq \sum_{n=0}^{L-1} 2^\gamma L^{2\gamma} \langle \Big(\frac{\sum_{k=1}^{2L-1-n} \sum_{i \in \mathcal{D}_k} \mu_i r_i}{2L^2} \Big)^\gamma \rangle$$

$$\geq \sum_{n=0}^{L-1} 2^{\gamma} L^{2\gamma} \frac{\sum_{k=1}^{2L-1-n} \sum_{i \in \mathcal{D}_k} \mu_i \langle r_i \rangle}{2L^2} = 2^{\gamma} L^{1+2\gamma} , \tag{3.55}$$

where the last inequality follows on observing that

$$\sum_{k=1}^{2L-1-n} \sum_{i \in \mathcal{D}_k} \mu_i = L^2.$$

Thus, for $r_i \leq 2$, the argument between the brackets is less than or equal to one. Furthermore, for any x and $\gamma \in [0,1]$, $x^{\gamma} \geq x$.

Equation (3.55) together with equation (3.51) gives

$$2^{\gamma} L^{1+2\gamma} \leq E_{rr}(\gamma) \leq E(\gamma) \sim L^{1+2\gamma} \tag{3.56}$$

and thus

$$E_{rr}(\gamma) \sim L^{1+2\gamma}. \tag{3.57}$$

And then one can conclude that

$$E_{rr}(\gamma) \sim \min(L^2, L^{1+2\gamma}), \tag{3.58}$$

and all the results of Section 3 hold.

We conclude the Chapter by resuming in the following table the universality classes which arise for different values of the parameter γ and in presence or absence of disorder in for the OCN model, together with models which share the same geometrical features.

τ	Φ	Ψ	d_l		
$\frac{4}{3}$	$\frac{3}{2}$	$\frac{3}{2}$	1	*Scheiddeger* *1d- random aggregation*	*OCN* $\gamma=1$ *(no disorder)*
$\frac{3}{2}$	2	2	1	*Peano basin* *mean field Scheiddeger*	*OCN* $1/2 < \gamma < 1$
$\frac{11}{8}$	2	$\frac{8}{5}$	$\frac{5}{4}$	*Random Spanning Trees*	*OCN* $\gamma = 0$
$\frac{7}{5}$	$\frac{5}{3}$	$\frac{5}{3}$	1	*Polymer in* *random enviroment*	*OCN* $\gamma = 1$ *(with disorder)*

Figure 3.2: The universality classes of OCN model, together with the models which share the same exponents

4 Numerical results

4.1 Global minima

Since Optimal Channel Network model has been introduced, extensive numerical simulations have been carried out by different authors to investigate the geometric properties of these structures. The aim was to understand to which extent the measured exponents for the power law tails of the distribution of cumulated areas and upstream length are sensitive of the topological feature imposed to the network, like for example the shape of the basin, the possibility for multiple outlet, the presence or the absence of links between second neighbors. Also the sensitivity to the different initial conditions from which the optimizations algorithm were started from has been considered and the data obtained compared with the ones coming from DEM of real rivers.

The most striking result of these works is that substantial differences arise in the values of measured exponents when 'crude' or more sophisticated algorithm are used; and while data coming from 'simpler' algorithm are in very good agreement with data coming from real rivers, the results obtained with sophisticated algorithm seems to be very close to the exact result discussed in the previous chapter.

In order to understand what this 'algorithm dependence' is due to and how much numerical results matches with our predictions, we performed a large number of simulations of OCN, mainly along two avenues:

i) the search for the global minimum with a Metropolis algorithm for $\gamma = 1/2$.

ii) the statistics over local minima for $\gamma = 1/2$; strikingly these yield consistent but different values for the scaling exponents. By a local minimum, we mean a configuration (a spanning tree) of the network such that no link can be changed without increasing the energy. The global minimum is of course also a local minimum; but in the two cases we found different statistics, that is suggestive of a very rich structure of the energy-landscape. We will postpone the results concerning the latter subject to the next Section, focusing our attention only on the scaling properties of the global minimum.

In the computer simulations we considered a square lattice with all sites on one side allowed to be an outlet for the network. Periodic boundary conditions were chosen in the other direction.

Once the simulation has been performed over the whole lattice, the basin with the biggest drained area is selected and only sites contained therein are used to calculate statistical quantities. Multiple outlets are allowed in order to minimize finite-size effects. The rainfall is assumed to be uniform over the whole lattice. The optimization method used is simulated annealing, in which a parameter T analogous to the temperature is introduced and lowered during the simulation. For each T value the system is relaxed in the following way: a new allowed configuration "near" the initial one ("near" means one differing from the previous one only in one link) is randomly chosen; the dissipation energy of the new configuration is calculated and compared with the value of the old one. The new configuration is accepted with probability 1 if ΔE is negative, and with probability $\exp[-\frac{\Delta E}{T}]$ otherwise.

In short a sketch of the algorithm is:

i) Generation of a random initial configuration:

Starting from a given, fixed tree we obtain a random initial configuration running steps *ii*) and *iii*) several times. In this way only changes preserving the spanning loopless structure are accepted.

ii) Random changes of the configuration:

We select randomly one site i and then again randomly one of the "free" (not yet belonging to the tree) links connected with i, if any.

iii) Geometrical controls:

The absence of a loop in the new configuration is checked. If a loop is present, step *ii*) is repeated.

iv) Energetic control:

The change, ΔE, in the dissipation energy dissipation is calculated. If it is negative we go on to step *v*). Otherwise, a random number p uniformly distributed in the interval $[0, 1]$ is generated and compared with $\exp[-\frac{\Delta E}{T}]$: if $\exp[-\frac{\Delta E}{T}] \leq p$ we go on to step *v*) , otherwise the change is rejected and we go back to step *ii*).

v) Recalculation of changed quantities:

All variables involved in the change are updated.

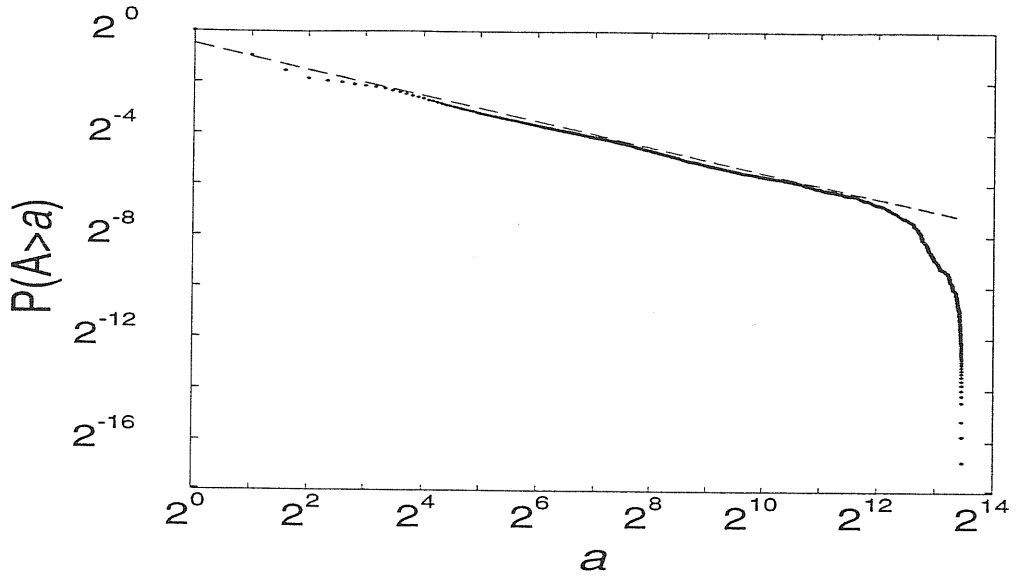

Figure 4.1: The distribution $P(A > a)$ versus a for a basin of linear size $L = 128$. Such a distribution has been obtained by mean of a Metropolis-like algorithm (attempting to seek the global minimum) and averaged over ten samples. The slope displayed is $1 - \tau = -0.50$.

vi) Lowering of the T parameter:

> In each cycle, the T parameter is decreased with the following rule: at the n-th cycle T is given by $T(n) = \alpha^n T(0)$, where α is a parameter very close to 1 (we choose $\alpha = 0.986$) and $T(0)$ is a suitable chosen constant.

After step *i*), steps *ii*)-*v*) are repeated many times, say N. Then we go to step *vi*) in which the T parameter is lowered and the entire algorithm (except step *i*)) is repeated. The annealing process stops when T reaches very low values ($\approx 10^{-4}$).

The simulations have been repeated varying the initial configuration for a size $L = 128$. The statistical quantities do not depend on the initial data. The integrated probability distributions for the accumulated areas and mainstream lengths averaged over 10 trials are shown in figure (4.1) and figure (4.2) and give $\tau = 1.50 \pm 0.02$ and $\psi = 2.00 \pm 0.02$ where the error is estimated as the root mean square root over the ten trials.

These results are in perfect agreement with equation (2.28) and confirm that the analytical results hold when $\gamma = 1/2$.

In effect, comparing one of the stable tree obtained with algorithm described above with a Peano basin we note that, apart differences at the smallest scales, they exhibit identical structures. We state then that with a very slow annealing it is possible to approach a tree which realize a value for the dissipated energy very close to the absolute minimum starting

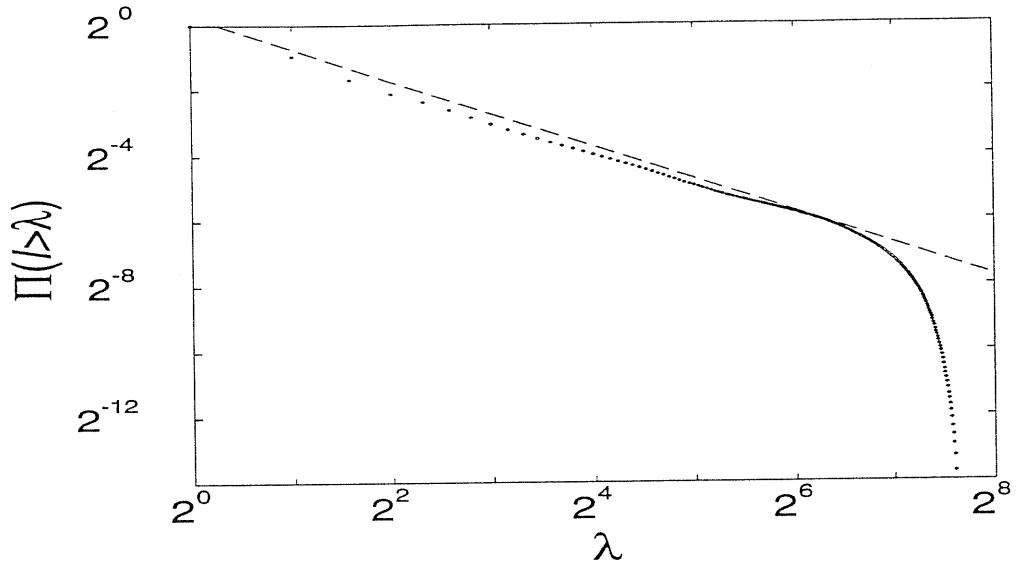

Figure 4.2: The distribution $\Pi(l > \lambda)$ versus l_0 for the same conditions as in Fig. 5. The slope $1 - \psi = -1.00$

from a generic configuration. These results can be compared with the ones obtained by Meakin et al. They allowed each site of the border to be an outlet and considered the distribution of accumulated areas of a site belonging to the border (and not for a generic site of the basin as we have been doing in the present paper). They found a power law behavior for such a distribution: $P_\partial(a) \sim a^{-\tau_\partial}$ with τ_∂ numerically estimated to be $\simeq 1.51$. If finite size scaling is invoked for such a distribution [32],

$$P_\partial(a, L) = a^{-\tau_\partial} f_\partial\left(\frac{a}{L^{1+H}}\right)$$

then, as in (2.11), one finds:

$$\langle a \rangle_\partial \sim L^{(1+H)(2-\tau_\partial)}.$$

As noted in [32] the mean accumulated area for a border site in a basin is just the number of sites in the bulk divided by the number of sites in the border. Denoting by D the fractal dimension of the border,

$$\langle a \rangle_\partial L^D \sim L^{(1+H)},$$

$\tau_\partial = 1 + \frac{D}{1+H}$. In the case of compact basins ($H = 1$), $\tau_\partial = 1 + \frac{D}{2}$, ($\tau_\partial = 3/2$ for a square). Note that τ_∂ is independent of the class of spanning tree chosen to drain the basin and it is *a priori* different from the τ we introduced to characterize the distribution of accumulated areas in the bulk, which we found to be for $H = 1$, $\tau = 2 - \frac{d_l}{2}$.

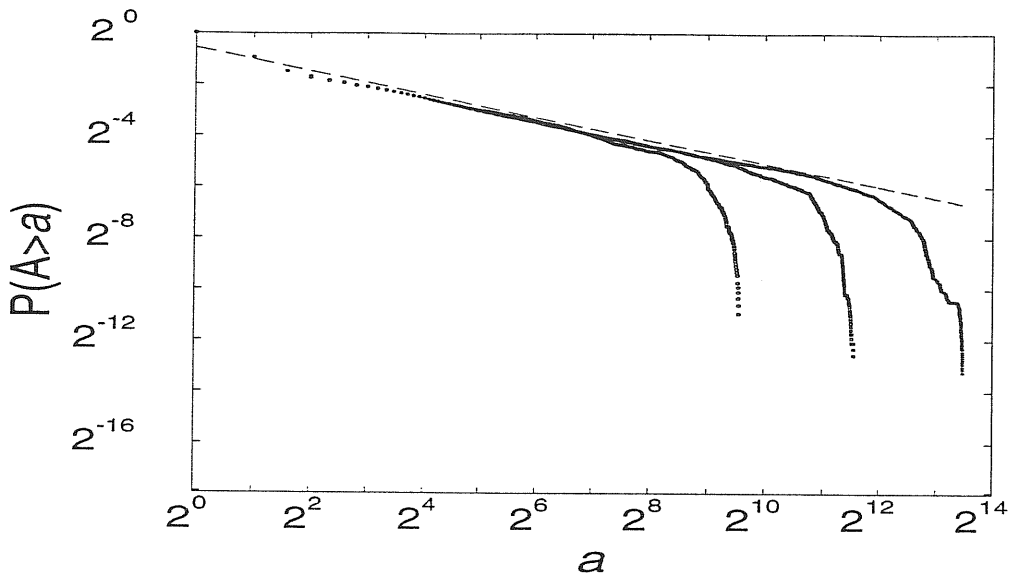

Figure 4.3: $P(A > a)$ versus a for three different sizes of the basin: $L = 32, L = 64$ and $L = 128$. Local minima are considered here, the distribution is obtained averaging over 40 samples. The slope is $1 - \tau = -0.45$

4.2 Local minima

We have performed the search for local minima with an algorithm equivalent to a $T = 0$ Metropolis scheme, i.e. one in which new configurations are accepted only if energetically favorable. The simulation has been repeated 40 times, starting with different, randomly chosen, initial data and varying the size L of the system: $L = 32, 64, 128$.

The values obtained for the characteristic exponents of the probability distribution considered above, τ and ψ are in very good agreement with experimental data. The distributions obtained starting from different initial condition do not substantially differ from one another, all yielding the same value for the exponents.

The statistical quantities thus seem to be robust with respect to variations of initial conditions, showing the self-averaging of the scaling parameters.

Results obtained averaging over 40 local minima are shown in figure (4.3) and in figure (4.4) and give $\tau = 1.45 \pm 0.02$ and $\psi = 1.82 \pm 0.02$.

The results are consistent with the scaling relations. A collapse test has been done to verify the consistency of numerical values of the exponents with the finite size scaling hypothesis (figure (4.5)).

We have performed the search for local minima with an algorithm equivalent to a $T = 0$ Metropolis scheme, i.e. one in which new configurations are accepted only if energetically

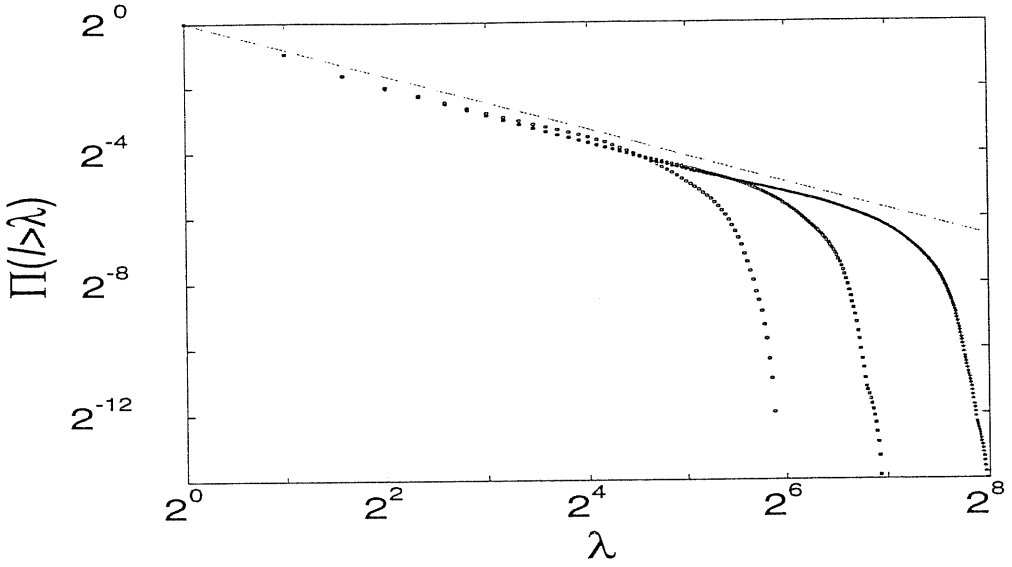

Figure 4.4: The same as in Fig. 7 for the upstream length distribution. The slope is $1 - \psi = -0.82$

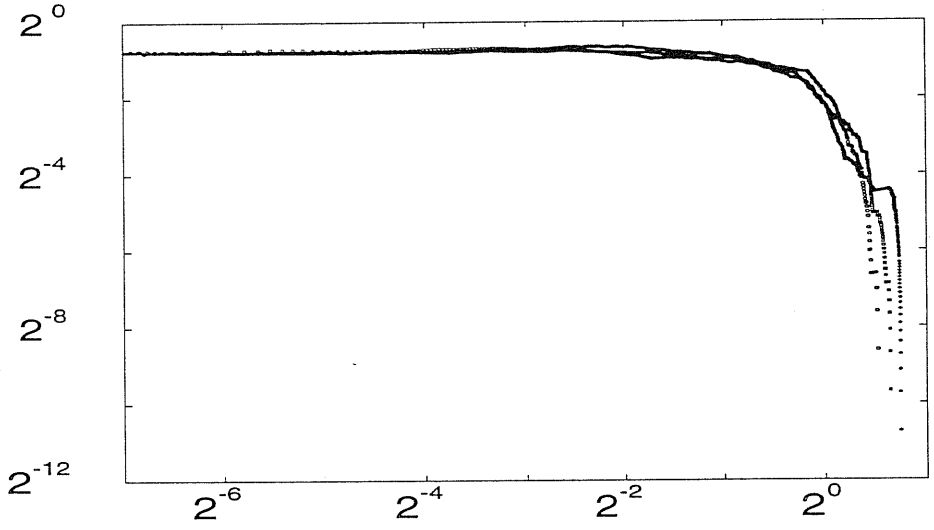

Figure 4.5: The result of the collapse test for the accumulated area distribution in the case of the local minima.

favorable. The simulation has been repeated 40 times, starting with different, randomly chosen, initial data and varying the size L of the system: $L = 32, 64, 128$.

The values obtained for the characteristic exponents of the probability distribution considered above, τ and ψ are in very good agreement with experimental data. The distributions obtained starting from different initial condition do not substantially differ from one another, all yielding the same value for the exponents.

The statistical quantities thus seem to be robust with respect to variations of initial conditions, showing the self-averaging of the scaling parameters.

Results obtained averaging over 40 local minima are shown in figures (4.3) and (4.4) and give $\tau = 1.45 \pm 0.02$ and $\psi = 1.82 \pm 0.02$. The results are consistent with the scaling relations. A collapse test has been done to verify the consistency of numerical values of the exponents with the finite size scaling hypothesis, see figure (4.5).

It is the case to remark that these values are very close to the experimental ones and that the tree which realize local minima are much more resemblant of the structure of DEM of real rivers than those which realize global minima.

The relevance of local minima can be supported also by the experiment run by Rinaldo and co-workers. They extracted from a DEM the shape of a real basin and searched for a local minimum in a lattice of that shape, getting a surprisingly good agreement between DEM and the OCN obtained.

The above discussion raise an important question: if, indeed, OCN model provide the mechanism which leads pattern formation in river basin, why global minimum need a so careful procedure to be approached and has got a structure so different from real rivers. while local minima are so close to them ? A possible answer could be that the 'energy landscape' for OCN model is very rich and 'rough', and very easily a searching algorithm (or Nature) can get trapped in a local minimum .

This qualitative observation can be supported by the following argument [49]: let's call S the set of all spanning trees over a given lattice of size L. For any configuration $s \in \mathcal{S}$ we define a Boltzmann-like probability of the tree s as:

$$P(s) \propto e^{-H_\gamma(s)/T} \tag{4.1}$$

where T^{-1} is the Gibbs' parameter mimicking the inverse of temperature of classic thermodynamic systems . For a fixed γ, let $H_\gamma(\mathcal{S})$ denote the finite set of all possible values that may be taken on by $H_\gamma(s)$ for trees $s \in \mathcal{S}$. Given an energy level, say $E \in H_\gamma(\mathcal{S})$, let $N(E)$ be the degeneracy, i.e. the number of different spanning trees s for which $H_\gamma(s) = E$. One therefore obtains

$$P(H_\gamma(s) = E) = \sum_{s:H_\gamma(s)=E} P(s) \propto N(E)exp(-E/T). \tag{4.2}$$

Defining the thermodynamic entropy as

$$\sigma(E) = logN(E), \tag{4.3}$$

one obtains:

$$P(H_\gamma(s) = E) \propto e^{-F(E)/T} \tag{4.4}$$

where a formal free energy $F(E) = E - T\sigma(E)$ has been introduced. Indeed, the most probable states correspond to an energy E that minimizes $F(E)$.

The claim is that the entropy scales sub-dominantly with system size compared to the energy so that even for a non zero value of the Gibbs' parameter the most probable spanning tree configurations determined by minimizing the free energy can be equally well obtained by minimizing the energy, provided that L is large enough. As a result, in the thermodynamic limit the system described by the probability in Eq. (4.4) always tends to operate at zero temperature, i.e. the total energy in Eq. (3.11) is minimized.

Our exact result is that for the set s of OCNs one has

$$E = \text{Min } H_\gamma(s) \propto L^{2+\delta} \tag{4.5}$$

where $\delta = 2\gamma - 1$ and then $\delta > 0$ for $\gamma > 1/2$.

The $\gamma = 1/2$ has $\delta = 0$, but with a logarithmic correction leading to an effective δ of $0.1-0.2$ as shown by detailed examination of data in computer studies of accessible local minima.

For spanning loopless trees the number $N(E)$ of configurations s with given energy E scales at most as $N(E) \propto \mu^{L^2}$, so that $S(E)$ scales at most as L^2, where μ is a real number depending on lattice properties and the energy. This follows from noting that the total number N of spanning trees is less then the number of possible ways of choosing $L^2 - 1$ links (number of link s in a spanning tree) among all the $2L(L+1)$ possible links. Thus

$$N < \binom{2L(L+1)}{L^2-1} \sim 2^{2L^2} \tag{4.6}$$

Since the number of configurations with a given energy is less then or equal to N, $N(E) \leq 2^{2L^2}$ and the above scaling of entropy is satisfied.

We conclude that for spanning trees (with $\gamma \geq 1/2$), the entropy scales sub-dominantly to the energy with system size and, in the thermodynamic limit $L \to \infty$, min $F(E) \propto L^{2+\delta}$ because $\delta > 0$. Hence the configuration s that minimizes H_γ also minimizes $F(E)$, whatever the Gibbs' parameter T^{-1}, provided the system is large enough. Hence OCNs, which correspond to the 0-temperature assumption (i.e. the configuration yielding min $F(E)$ is that with min E only for $T \to 0$), reproduce natural conditions at any temperature for large L.

We suggest that this is the reason for the outstanding ability [15] ,[14] of OCNs to reproduce observational evidence regardless of diversities in surface lithology, geology, vegetation or climate. This also strongly suggests that size effects of samples of real networks may lead to spurious results for small sizes [50].

These considerations lead to the formulation of the principle of Feasible Optimality [51] according which Nature is unable to reach the true ground state when complex systems are involved with optimization problems. Optimization just stops when a local minima is reached; moreover these class of local minima can exhibit its ow peculiar characteristics that are definitively different from those of global minima.

We conclude noting that a similar behavior has been recently observed in other physical systems. In [51] has been studied numerically a 2-dimensional Ising system with a weak disorder in the interaction and where border spins have been fixed to have opposite orientations on different sides. $T = 0$ dynamics was run from a generic initial configuration. When a stable stationary configuration has been reached they studied the geometrical properties of the interface between regions containing spins with different orientation. They found for this interface a well defined self-similar behavior characterized however by scaling exponents which resulted to be unambiguously different from the ones obtained with a $T \neq 0$ dynamic.

Bibliography

[1] L. B. Leopold and W. B. Langbein, U. S. Geol. Surv. Prof. Pap. **500-A**, (1962).

[2] D. R. Montgomery and W. E. Dietrich, Nature **336**, 232 (1988).

[3] D. R. Montgomery and W. E. Dietrich, Science **255**, 826 (1992).

[4] D. G. Tarboton, R. L. Bras, and I. Rodriguez-Iturbe, Water Resour. Res. **25**, 2037 (1989).

[5] L. B. Leopold, M. Wolman, and J. Miller, *Fluvial Process in Geomorphology* (Freeman and Co, San Francisco, 1964).

[6] S. A. Schumm, *The Fluvial System* (J. Wiley, New York, 1977).

[7] L. E. Band, Water Resour. Res. **22(1**, 15 (1986).

[8] D. G.Tarboton, R. Bras, and I. R. Iturbe, Parson Lab. Rep. no. 386, Dep. Civ. Eng. MIT, Cambridge, Mass. , 251 (1986).

[9] J. T. Hack, U. S. Geol. Surv. Prof. Paper **294-B**, (1957).

[10] B. B. Mandelbrot, *The Fractal Geometry of Nature* (Freeman, New York, 1983).

[11] P. L. Barbera and R. Rosso, Water Resour. Res. **25**, 735 (1989).

[12] S. P. Breyer and R. S. Snow, Geomorphology **5**, 143 (1992).

[13] D. G. Tarboton, R. L. Bras, and I. Rodriguez-Iturbe, Water Resour. Res. **24**, 1317 (1988).

[14] I. Rodriguez-Iturbe *et al.*, Geophys. Res. Lett. **19**, 889 (1992).

[15] I. Rodriguez-Iturbe *et al.*, Water Resour. Res. **28**, 1095 (1992).

[16] A. Maritan *et al.*, Phys. Rev. E **53**, 1510 (1996).

[17] M. E. Fisher, *in Critical Phenomena, Proc. 51st Enrico Fermi Summer School, Varenna* (M. S. Green (Academic Press, New York, 1972).

[18] M. E. Fisher and B. M.N., Phys. Rew. Lett. **28**, 1516 (1972).

[19] M. N. Barber, *in Phase Transitions and Critical Phenomena, Vol.8* (C.Domb and J. L. Lebowitz (Academic Press), London, 1983).

[20] A. E. Scheiddeger, Bull. Assoc. Sci. Hydrol. **12**, 15 (1967).

[21] M. Takayasu, H. Takayasu, and Y. H. Taguchi, Int. J. Mod. Phys. B **8**, .

[22] H. Takayasu, M. Takayasu, A. Provata, and G. Huber, J. Stat. Phys. **65**, 725 (1991).

[23] A. Marani, R. Rigon, and A. Rinaldo, Water Resour. Res. **21**, 3041 (1991).

[24] A. Flammini and F. Colaiori, to appear on Journal of Physics A , .

[25] A. Coniglio, Phys. Rew. Lett. **62**, 3054 (1989).

[26] S. S. Manna, D. Dhar, and S. N. Majumdar, Phys. Rev. A **46**, R4471 (1992).

[27] D. M. Gray, J. Geophys. Res. **66**, 1215 (1961).

[28] W. Langbein, .S. Geol. Surv. Prof. Paper **968-C**, 1 (1947).

[29] J. Muller, Geol. Soc. A Bull. **84**, 3127 (1973).

[30] F. Colaiori, A. Flammini, A. Maritan, and J. R. Banavar, submitted to PRE , (1996).

[31] R. Rigon *et al.*, **to appear in Water Resour. Res.**, .

[32] P. Meakin, J. Feder, and T. Jossang, Physica A **176**, 409 (1991).

[33] G. Huber, Physica A **170**, 463 (1991).

[34] A. Giacometti, A. Maritan, and A. Stella, Int. Jour. Mod. Phys. B **B5**, 709 (1991).

[35] M. Nauenberg, Jour. Phys. A .

[36] T. Nieneijer and J. M. J. V. Leeuwen, in Phase Transition and Critical Phenomena .

[37] A. Maritan, F. Colaiori, A. Flammini, and J. R. Banavar, Science **272**, 984 (1996).

[38] Kirkchoff, Ann. Phys. Chem. **72**, 497 (1847).

[39] C. M. Fortuin and P. W. Kasteleyn, Physica **57**, 536 (1972).

[40] S. N. Majumdar and D. Dhar, Physica A **185**, 129 (1992).

[41] S. S. Manna, D. Dhar, and M. S. N., Phys. Rev. A **46**, R4471 (1992).

[42] P. S. Stevens, *Patterns in Nature* (Brown and Co., Boston, 1974).

[43] P. G. Doyle and J. L. Snell, *Random Walks and Electric Networks* (American Math. Soc., Darthmouth, 1984).

[44] F. Colaiori, Ph. D. Thesis SISSA Trieste .

[45] A. Maritan, J. R. Banavar, F. Colaiori, and A. Flammini, in preparation , .

[46] D. A. Huse and C. L. Henley, Phys. Rev. Lett. .

[47] M. Kardar, Phys. Rev. Lett. **55**, 2923 (1985).

[48] D. A. Huse, C. L. Henley, and D. S. Fisher, Phys. Rev. Lett. **55**, 2924 (1985).

[49] Rinaldo *et al.*, Phys. Rev. Lett. **76**, 3364 (1996).

[50] B. M. Troutman and M. R. Karlinger, Water Resour. Res. **29**, 1213 (1994).

[51] A. Rinaldo *et al.*, submitted . .